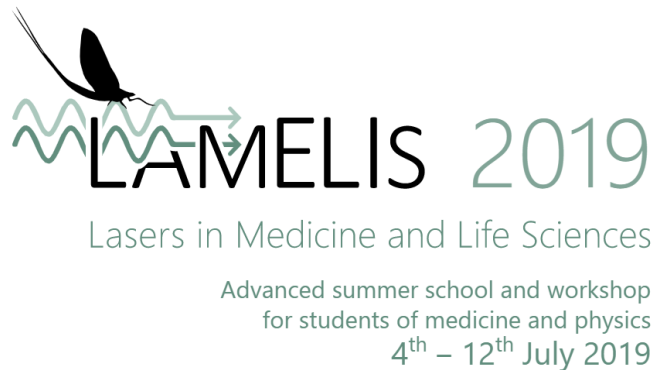


TOTAL INTERNAL REFLECTION FLUORESCENCE MICROSCOPY TIRFM

principles & applications



Beáta Bugyi
University of Pécs – Medical School
Department of Biophysics



UNIVERSITY OF PÉCS – MEDICAL SCHOOL – DEPARTMENT OF BIOPHYSICS
CYTOSKELETAL DYNAMICS LAB

<http://cytoskeletaldynamics.wix.com/mysite>

INTRODUCTION

OVERVIEW

INTRODUCTION

- Classic and advanced resolution in the fluorescence microscope

TOTAL INTERNAL REFLECTION FLUORESCENCE MICROSCOPY

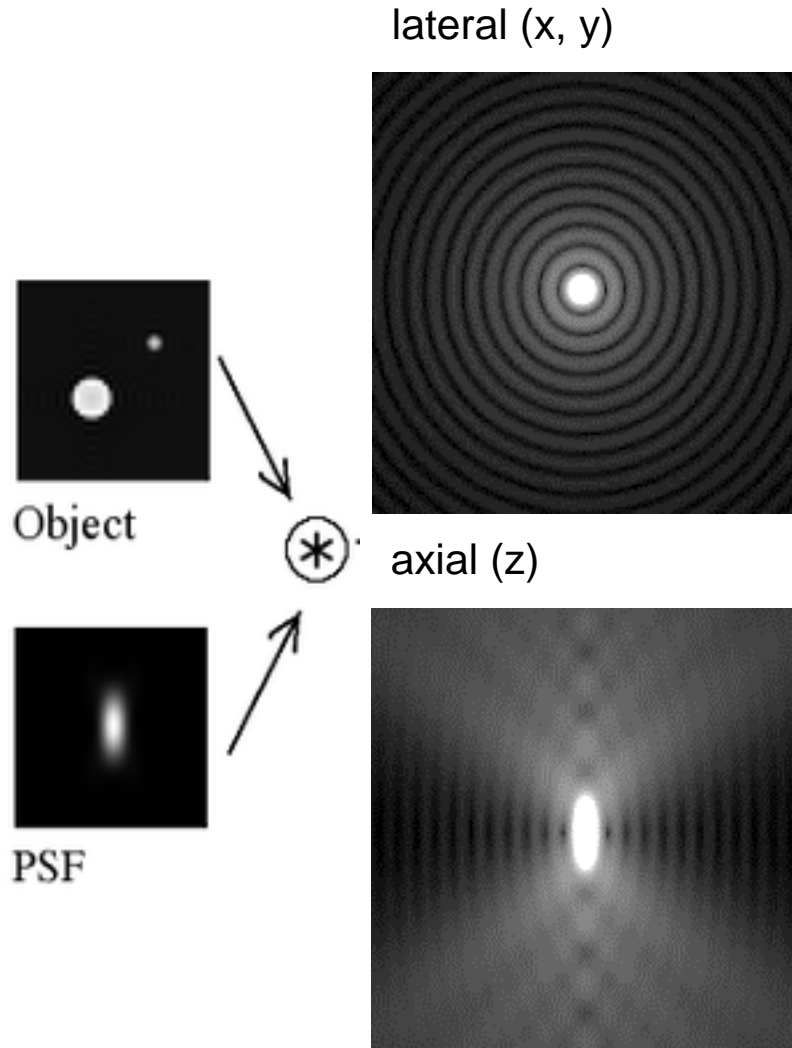
- Historical perspectives
- Physical principles
- How to set up a TIRF microscope?
- What TIRFM can/cannot do?
- Troubleshooting

APPLICATIONS

- Cell biology applications
- Protein biochemistry applications

Classic - resolution limited - fluorescence microscopy

- The resolution of the light microscope – how small things can be discerned – is intrinsically limited by the wave nature of light.
- Resolution/diffraction limit (19th century: Ernst Abbe, Lord Rayleigh)



object (ideal point) \rightarrow image (3D structure)

$$image = object \otimes PSF + noise$$

PSF = point spread function ~ distortion

$$object \sim \lambda \text{ (400 – 800 nm)}$$

Lateral resolution limit

$$d_{xy} = 0.61 \frac{\lambda}{NA} \sim \mathbf{200 \text{ nm}}$$

Axial resolution limit

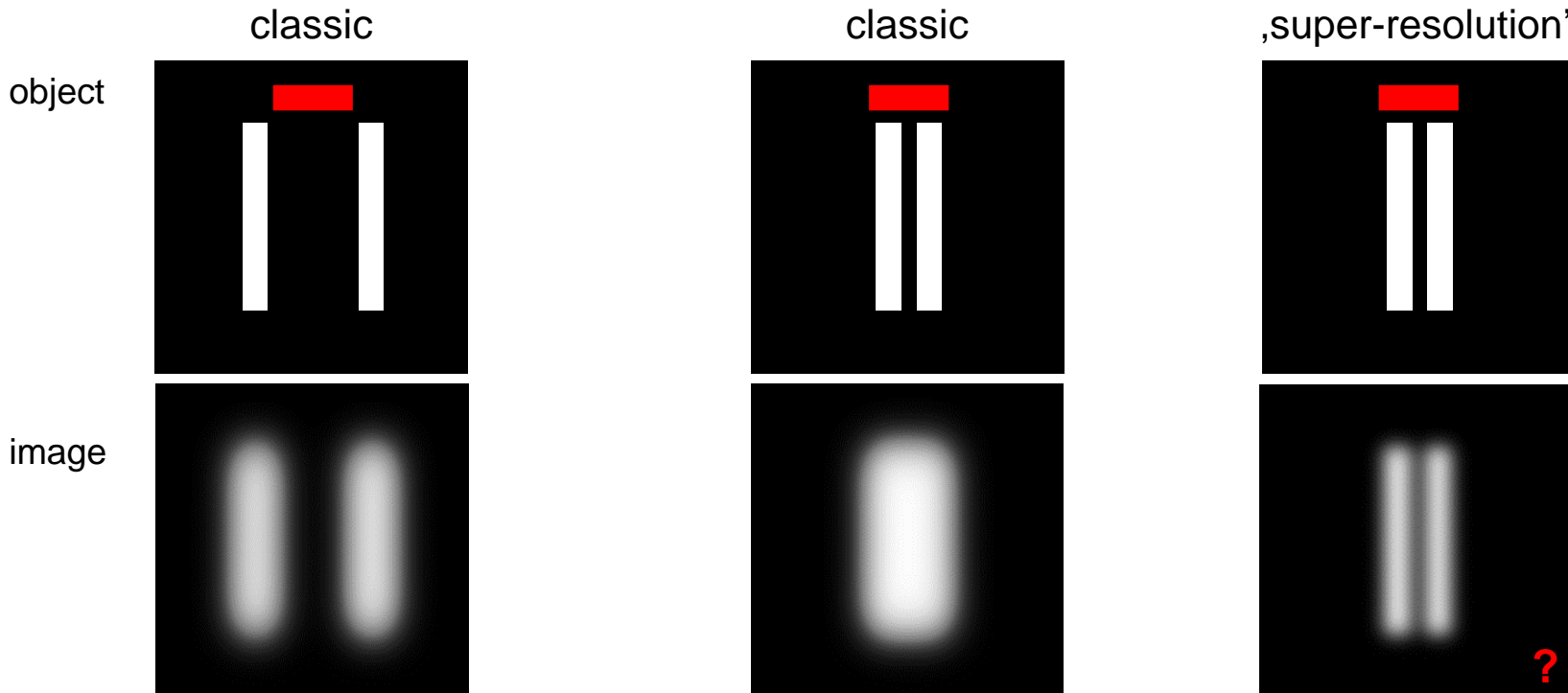
$$d_z = 2n \frac{\lambda}{(NA)^2} \sim \mathbf{800 \text{ nm}}$$

$$NA = n \times \sin \alpha$$

numerical aperture

Classic vs super-resolution fluorescence microscopy

Limit of resolution: $d_{xy} \sim 200 \text{ nm}$ ■



Classic fluorescence microscopy cannot achieve a resolution better than that is defined by the diffraction limit.

Super-resolution microscopy by surpassing the diffraction limit can provide better resolution than that is defined by the diffraction limit.

Classic vs super-resolution fluorescence microscopy

1873 diffraction limit

Ernst Abbe



2014 Nobel Prize in Chemistry

"for the development of super-resolved fluorescence microscopy"



Stefan Hell



Eric Betzig



William Moerner

Around 2000 Eric Betzig and William E. Moerner helped create a method in which fluorescence in individual molecules is steered by light. An image of very high resolution is achieved by combining images in which different molecules are activated.

In 1994, Stefan W. Hell developed a method in which one light pulse causes fluorescent molecules to glow, while another causes all molecules except those in a very narrow area to become dark. An image is created by sweeping light along the sample.

http://www.nobelprize.org/nobel_prizes/chemistry/laureates/2014/



Resolution improvement in fluorescence microscopy – overview

FLUORESCENCE MICROSCOPY (1911) – diffraction limited

CONFOCAL MICROSCOPY (1961)

- conjugate planes – filtering out-of-focus emission (~ 500 – 600 nm)
Minsky, M. Microscopy Apparatus. US Patent 3,013,467 (1961)

SUPER-RESOLUTION FLUORESCENCE MICROSCOPY

TOTAL INTERNAL REFLECTION FLUORESCENCE MICROSCOPY – TIRFM (1981)

- evanescent wave illumination – eliminate background fluorescence (~ < 100 nm)
Axelrod, D. Cell-substrate contacts illuminated by total internal reflection fluorescence. *J. Cell Biol.* 89, 141–145 (1981)


STIMULATED EMISSION DEPLETION MICROSCOPY – STED (2000)

- stimulated emission of fluorescence – PSF engineering (~ tens of nm)
 **Klar, T. A., Jakobs, S., Dyba, M., Egner, A., Hell, Stefan.** W. Fluorescence microscopy with diffraction resolution barrier broken by stimulated emission. *Proc. Natl Acad. Sci. USA* **97**, 8206–8210 (2000)

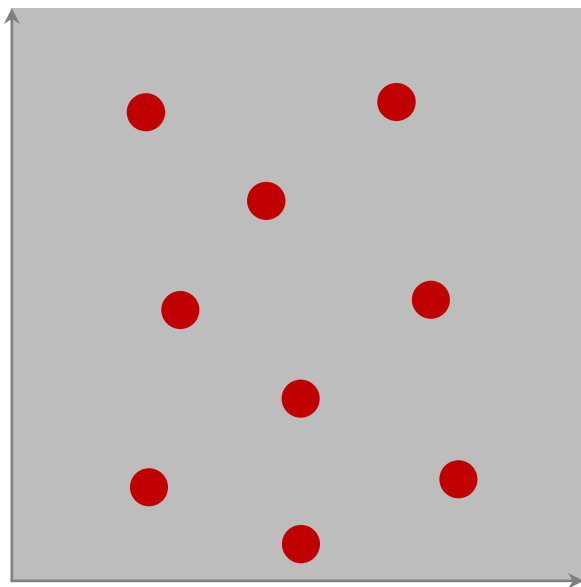
STRUCTURED ILLUMINATION MICROSCOPY – SIM (2000)

- spatially structured illumination/frequency mixing – extend frequency region (~ 100 nm)
Gustafsson, M. G. L., D. A. Agard, and J. W. Sedat. 2000. Doubling the lateral resolution of wide-field fluorescence microscopy using structured illumination. *Proc. SPIE.* 3919:141–150.
Gustafsson, M. G. L. 2000. Surpassing the lateral resolution limit by a factor of two using structured illumination microscopy. *J. Microsc.* 198:82–87.

SINGLE MOLECULE LOCALIZATION MICROSCOPY – STORM, PALM (2006)

- phototransformable fluorophores – Gaussian fit of PSF (~ tens of nm)
 **Betzig, Eric.** *et al.* Imaging intracellular fluorescent proteins at nanometer resolution. *Science* **313**, 1642–1645 (2006)
Rust, M. J., Bates, M. & Zhuang, X. Sub-diffractionlimit imaging by stochastic optical reconstruction microscopy (STORM). *Nature Methods* **3**, 793–796 (2006)
Dickson RM, Cubitt AB, Tsien RY and Moerner William (1997) On/off blinking and switching behaviour of single molecules of green fluorescent protein. *Nature* 388:355-358.

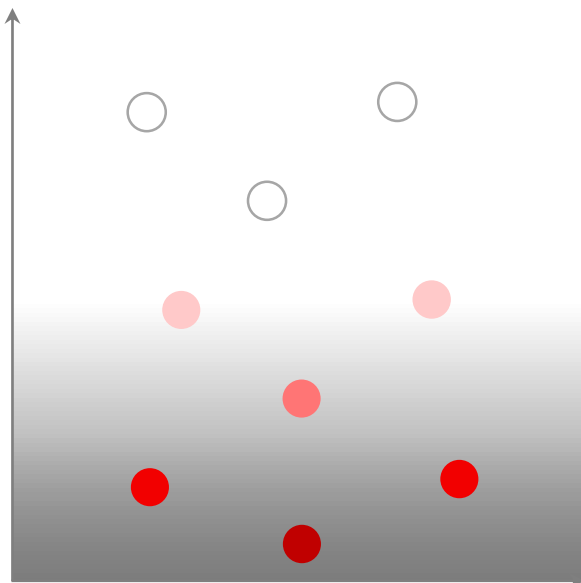
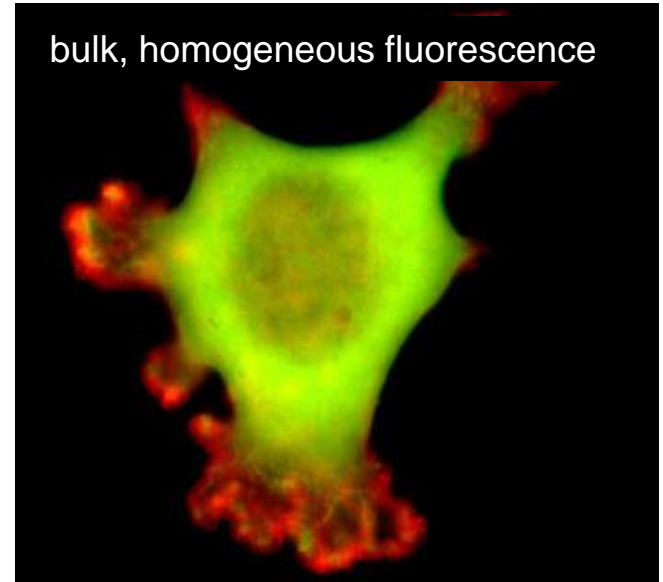
Excitation/emission patterns of fluorophores in WF and TIRF modes



WIDE-FIELD (WF)

illuminates the entire
thickness $\sim \mu\text{m}$

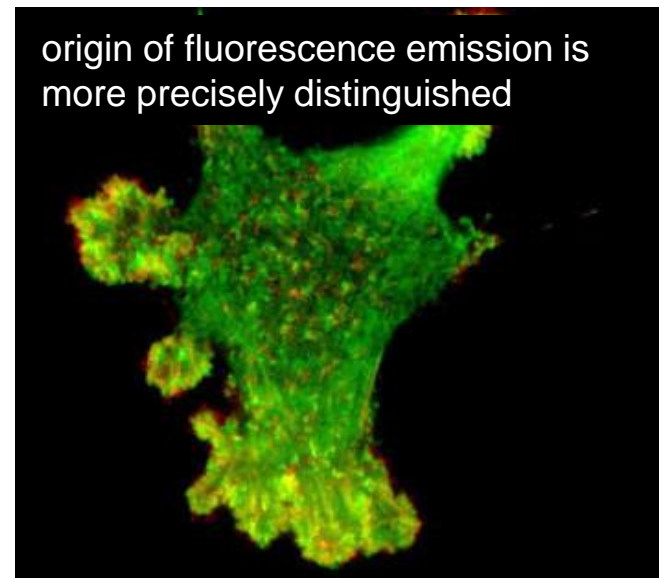
bulk, homogeneous fluorescence



TIRF

selectively illuminates the most
superficial layer $\sim 100 \text{ nm}$

origin of fluorescence emission is
more precisely distinguished



B16/F1 mouse skin melanoma cell

EGFP-myosin mRFP-actin

Introducing the concept of TIR in light microscopy

E. J. Ambrose
Nature 1956

„In order to study the contacts formed between cells and solid surfaces, it is possible to make use of the **slight penetration of light waves into the less dense medium when totally internally reflected** at the glass/water interface.”

SURFACE CONTACT MICROSCOPE

nonfluorescent, evanescent light scattering from cells

1194

NATURE November 24, 1956 VOL. 178

crease with duration of the heating, the radioactive yield into purified *p*-nitro benzoic acid is likely to be much less than 44 per cent in the second case.

After purification, and removal of the activity from the carboxyl group, the overall yield was about 70 per cent by weight (17 per cent by activity), the specific activity being 230 mc./gm.

Further studies on the use of this material are in progress. A detailed account of the method will be published elsewhere.

J. E. S. BRADLEY

Physics Department,
Middlesex Hospital Medical School,
London, W.1.
Sept. 7.

¹ Ingold, C. K., Ralsin, C. G., and Wilson, C. L., *Nature*, 134, 734 (1934).

² Best, A. P., and Wilson, C. L., *J. Chem. Soc.*, 239 (1946).

³ Gold, V., and Satchell, D. P. N., *J. Chem. Soc.*, 3609 (1955).

⁴ Gold, V., and Satchell, D. P. N., *J. Chem. Soc.*, 3622 (1955).

⁵ Koizumi, M., and Titani, T., *Bull. Chem. Soc. Japan*, 13, 318 (1938).

A Surface Contact Microscope for the study of Cell Movements

The study of the contacts formed by moving cells and solid surfaces, controlling their behaviour has been clearly shown in the phenomenon of contact guidance described by Weiss¹ and in contact inhibition described by Abercrombie and Heaysman².

In order to study the contacts formed between cells and solid surfaces, it is possible to make use of the slight penetration of light waves into the less dense medium when totally internally reflected at a glass/water interface. The apparatus used for these studies is illustrated in Fig. 1. Light from an intense source *S* (compact-source mercury arc) passes through the slit *T* and strikes the upper surface *A* of the 60°-prism. A cell suspension in water is mounted between an ordinary microscope slide and a coverslip and is sealed with immersion oil on the upper face of the prism (Fig. 2). The incident light now strikes the upper surface of the glass slide at an angle greater than the critical angle and is totally internally reflected at the glass/water interface. In reality the beam penetrates the less dense medium slightly, as shown diagrammatically in Fig. 3(a). If a cell of refractive index greater than water is moving on

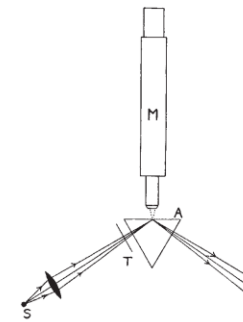


Fig. 1

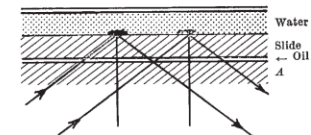


Fig. 2

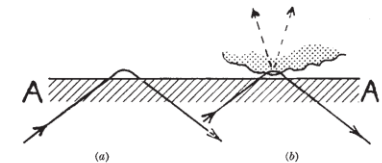


Fig. 3

the surface (Fig. 3(b)), those portions which make close contact with the surface of the glass will enter the penetrating beam and will scatter the light, owing to the presence of minute inhomogeneities in their structure.

When seen from above, through the microscope *M*, the field appears completely dark, provided that the incident light beam has been carefully shielded and the prism faces are clean. But those regions of the moving cells which are in close contact with the glass are brightly illuminated. In addition, the actual contours of the cell surface can be explored by changing the angle of the incident beam. With increasing angle, the degree of penetration of the incident beam is decreased so that the areas of the cell which are illuminated are reduced, eventually to those regions which are almost in molecular contact with the glass surface.

The effect is particularly well illustrated in the case of a filamentous mould kindly provided by Dr. R. J. Goldacre. As the mould moves forward along the glass, bright waves of light can be seen to move rapidly along its length, which are due to continuous changes in the points of adhesion between the lower surface of the mould and the glass surface. Apart from its biological application, the microscope may prove to be generally useful for the study of a number of phenomena, particularly those connected with the forces of cohesion between surfaces.

I am grateful to Prof. A. Haddow for his interest and encouragement in this work. This investigation has been supported by grants to the Chester Beatty Research Institute (Institute of Cancer Research: Royal Cancer Hospital) from the British Empire Cancer Campaign, Jane Coffin Childs Memorial Fund for Medical Research, the Anna Fuller Fund and the National Cancer Institute of the National Institutes of Health, U.S. Public Health Service.

E. J. AMBROSE

Chester Beatty Research Institute,
Institute of Cancer Research:
Royal Cancer Hospital,
London, S.W.3.
July 27.

¹ Weiss, P., "Principles of Development" (Henry Holt and Co., New York, 1939).

² Abercrombie, M., and Heaysman, J. E. M., *Exp. Cell Res.*, 5, 111 (1953); 6, 293 (1954).

Daniel Axelrod Journal of Cell Biology 1981

„The new method is an application ... and **extension to fluorescence of the total internal reflection microscope illumination system introduced by Ambrose.**”

Cell-Substrate Contacts Illuminated by Total Internal Reflection Fluorescence

DANIEL AXELROD

Biophysics Research Division and Department of Physics, University of Michigan, Ann Arbor, Michigan 48109

ABSTRACT A technique for exciting fluorescence exclusively from regions of contact between cultured cells and the substrate is presented. The technique utilizes the evanescent wave of a totally internally reflecting laser beam to excite only those fluorescent molecules within one light wavelength or less of the substrate surface. Demonstrations of this technique are given for two types of cell cultures: rat primary myotubes with acetylcholine receptors labeled by fluorescent α -bungarotoxin and human skin fibroblasts labeled by a fluorescent lipid probe. Total internal reflection fluorescence examination of cells appears to have promising applications, including visualization of the membrane and underlying cytoplasmic structures at cell-substrate contacts, dramatic reduction of autofluorescence from debris and thick cells, mapping of membrane topography, and visualization of reversibly bound fluorescent ligands at membrane receptors.

The regions of contact between a tissue culture cell and a solid substrate are of considerable interest in cell biology. These regions are obvious anchors for cell motility (1), loci for aggregation of specific membrane proteins (2-4), and convergence points for cytoskeletal filaments (2, 5, 6). Described here is a fluorescence microscope method for selectively visualizing specific molecules in cell-substrate contact regions while avoiding fluorescence excitation of the cell interior liquid medium and cellular debris. Other potential applications of this method include viewing fluorescence-marked receptors at very low cell surface concentrations, cytoplasmic filaments in thick cells, and fluorescent agonists that bind reversibly to the cell membrane.

The new method is an application of total internal reflection fluorescence (TIRF) to cellular microscopy and is an extension to fluorescence of the total internal reflection microscope illumination system introduced by Ambrose (7) to detect light scattered at cell-substrate contacts. TIRF microscopy utilizes a light beam in the substrate that is obliquely incident upon the substrate liquid interface at an angle greater than the critical angle of refraction. At this angle, the light beam is totally reflected by the interface. However, an electromagnetic field called the "evanescent wave" does penetrate into the liquid medium. The evanescent wave propagates parallel to the surface with an intensity I that decays exponentially with perpendicular distance z from the surface:

$$I = I_0 \exp(-z/d) \quad (1)$$

The characteristic exponential decay depth d is:

$$d = \frac{\lambda}{4\pi n_2} \left(\frac{\sin^2 \theta}{\sin^2 \theta_c} - 1 \right)^{-1/2} \quad (2)$$

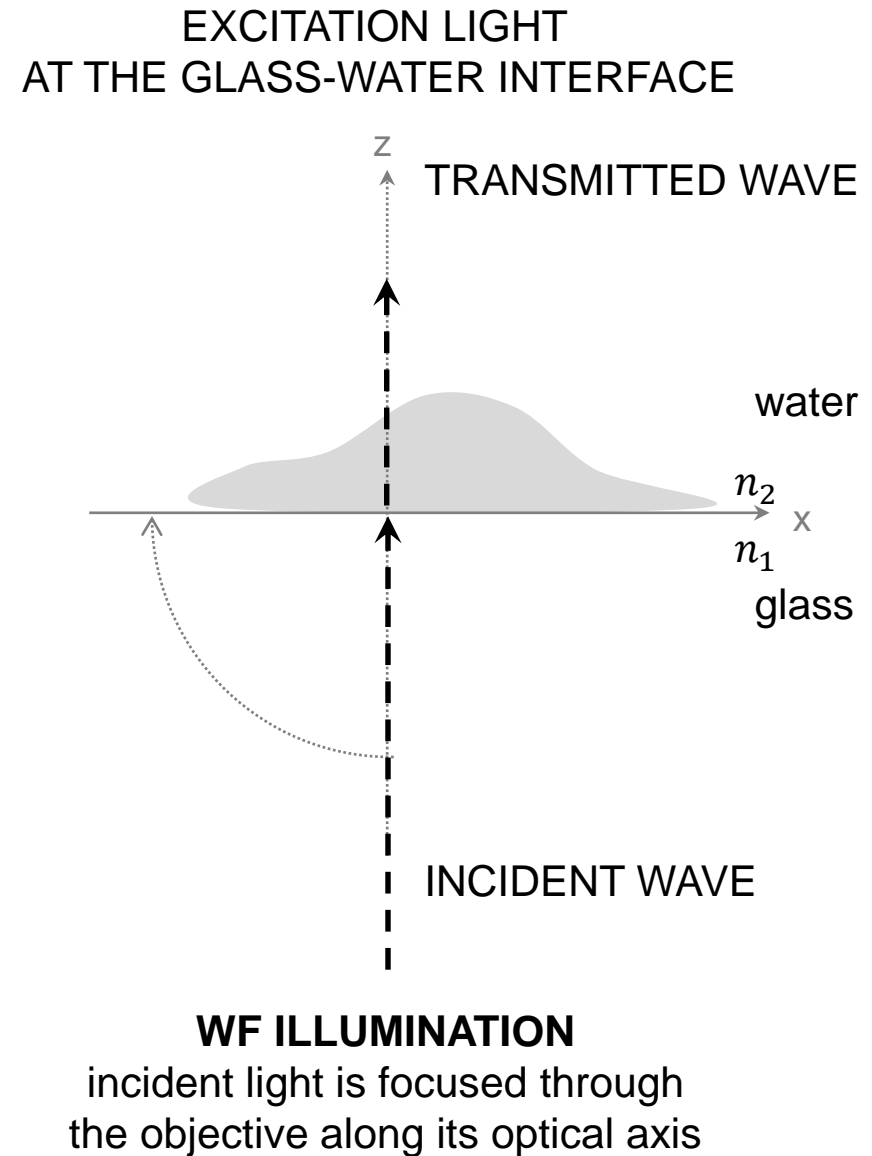
where n_1 = refractive index of the substrate; n_2 = refractive index of the liquid medium; θ_c = the critical angle of incidence = $\sin^{-1} n_2/n_1$; θ = the angle of incidence, $\theta > \theta_c$; and λ = the wavelength of incident light in vacuum. The decay depth d decreases with increasing θ . Except for θ close to θ_c (where $d \rightarrow \infty$), d is on the order of λ or smaller. I_0 , the intensity of the evanescent wave at $z = 0$, is on the order of the incident light intensity except for angles of incidence very near the critical angle (8). Therefore, for most experimental configurations, a fluorescent molecule located in the evanescent wave at $z = 0$ will be excited with roughly the same efficiency as it would if it were located in the incident beam.

A fluorescent molecule located close to the surface in the evanescent wave can become excited and emit fluorescence; molecules much farther away will not be excited. The efficiency of excitation decays exponentially according to Eqs. 1 and 2. For typical experiments described here, identical fluorescent molecules located at 1, 10, 100, and 1,000 nm from the surface will emit relative fluorescence intensities of 0.99, 0.92, 0.43, and 0.0002, respectively. For cells adhering to the surface, only fluorescent molecules at or near the cell surface in the regions of closest contact with the substrate will be excited significantly.

TIRF has been employed previously to study surface interactions in a variety of molecular systems, including solutions of fluorescein (9) and serum albumin (10, 11) at glass surfaces, and antibodies at antigen coated surfaces (12). More recently, TIRF has been combined with fluorescence photobleaching recovery and fluorescence correlation spectroscopy to study the surface adsorption/desorption kinetics of fluorescent macromolecules (13, 14) and viruses (15).

A completely unrelated transmitted illumination technique,

Traditional wide-field illumination



Total internal reflection – geometrical optical principles

SNELL'S LAW OF REFRACTION

$$n_1 \sin \alpha_1 = n_2 \sin \alpha_2$$

glass ($n_1 = 1.515$) > water ($n_2 = 1.333$) interface
angle of incidence (α_1) < angle of refraction (α_2)

CRITICAL ANGLE

angle of refraction (α_2) = 90°
angle of incidence (α_1) $\equiv \alpha_{critical}$

$$\frac{n_1}{n_2} \sin \alpha_{critical} = 1$$

$$\sin \alpha_{critical} = \frac{n_2}{n_1} = \frac{1.333}{1.515} = 0.88$$

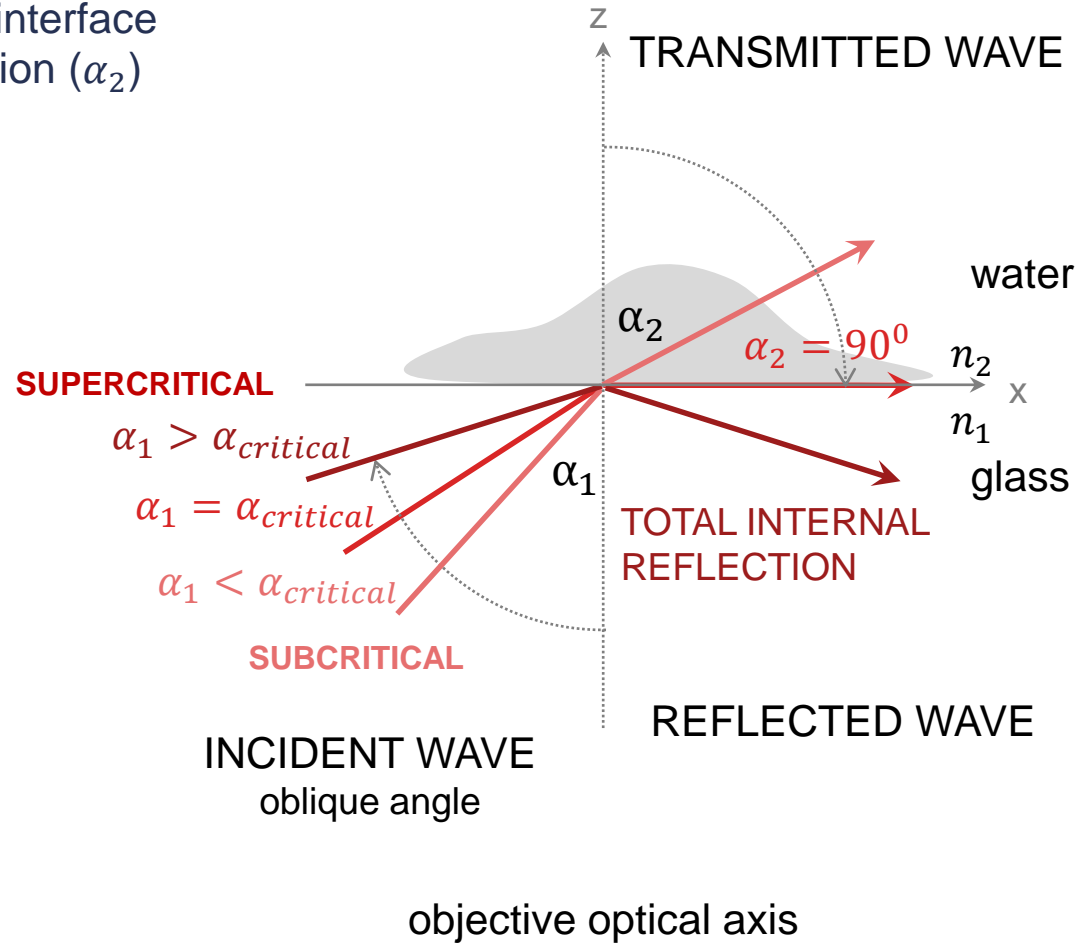
$$\alpha_{critical} = 61.63^\circ$$

Notation:

1: incident wave/1st medium

2: transmitted wave/2nd medium

EXCITATION LIGHT AT THE GLASS-WATER INTERFACE



Total internal reflection – wave optical principles

Intensity response of fluorophores as a function of α_1

single refractive index change

monochromatic plane wave

INCIDENT: $\vec{E}_1(\vec{r}, t) = \vec{E}_1 \exp [i(\vec{k}_1 \vec{r} - \omega t)]$

TRANSMITTED: $\vec{E}_2(\vec{r}, t) = \vec{E}_2 \exp [i(\vec{k}_2 \vec{r} - \omega t)] =$

$= \vec{E}_2 \exp [i(k_2 \sin \alpha_2 x + k_2 \cos \alpha_2 z - \omega t)]$

$$ik_2(\sin \alpha_2 x + \cos \alpha_2 z) = ik_2 \left(\frac{\sin \alpha_1}{n} x + i \sqrt{\frac{\sin^2 \alpha_1}{n^2} - 1} z \right)$$

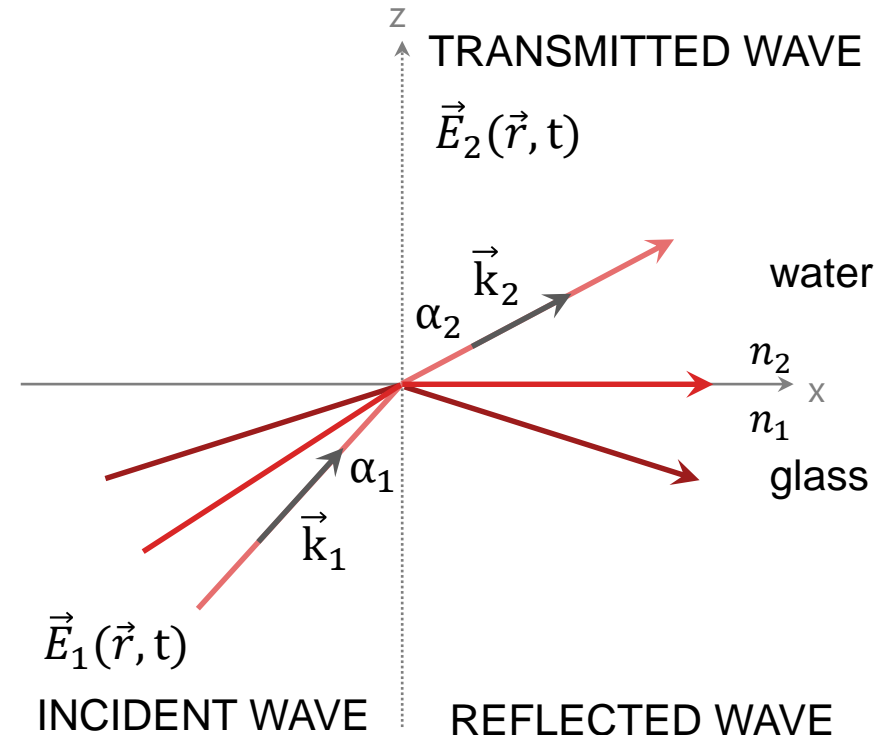
CRITICAL: $\alpha_1 = \alpha_c$

$\vec{E}_2(\vec{r}, t) = \vec{E}_2 \exp [i(k_2 x - \omega t)]$

SUPERCritical: $\alpha_1 > \alpha_c$

$\vec{E}_2(\vec{r}, t) =$

$$= \vec{E}_2 \exp \left[i \left(k_2 \frac{\sin \alpha_1}{n} x - \omega t \right) \right] \cdot \exp \left[-k_2 \sqrt{\frac{\sin^2 \alpha_1}{n^2} - 1} z \right]$$



Upon TIR an EM field appears in the second medium right above the surface.

The transmitted wave

- propagates perpendicular to the surface (z direction)
- attenuated exponentially = EVANESCENT („disappear in space')

Total internal reflection – evanescent field

EVANESCENT WAVE

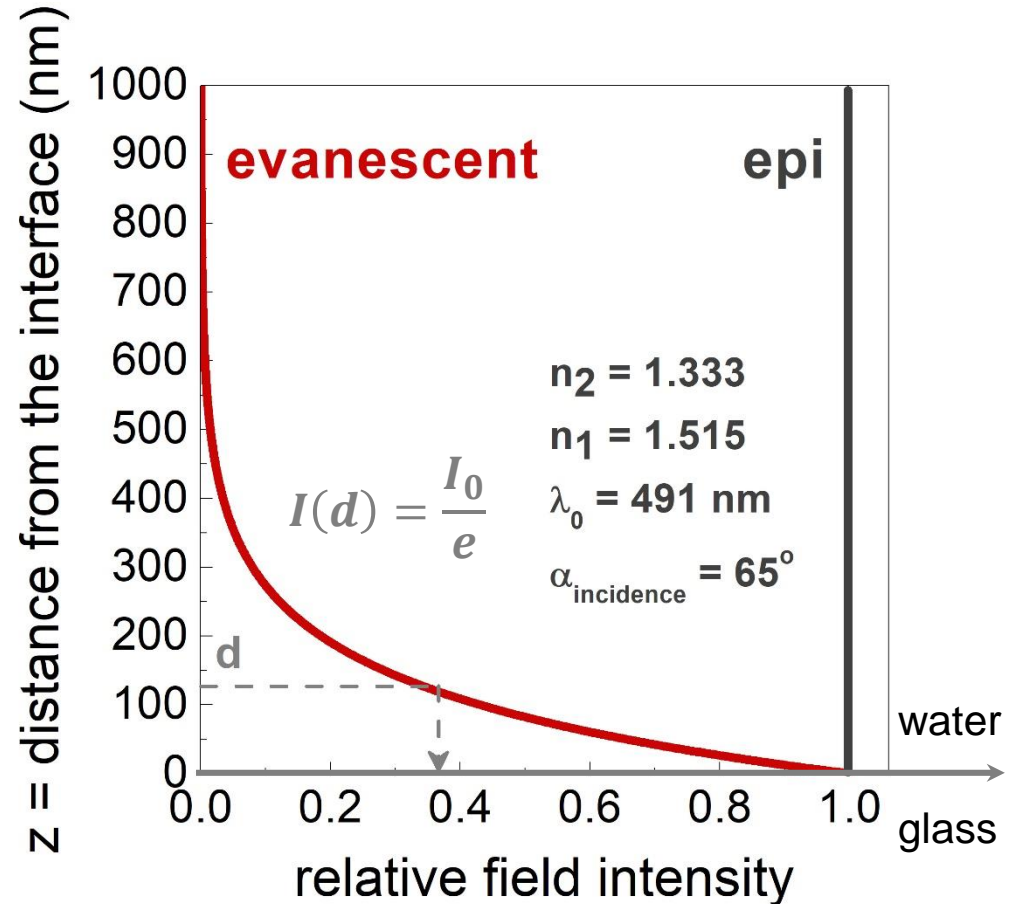
$$\begin{aligned}\vec{E}_{\text{evanescent}}(\vec{r}, t) &= \vec{E} \exp\left[-k_2 \sqrt{\frac{\sin^2 \alpha_1}{n^2} - 1} z\right] \\ &= \vec{E} \exp\left[-\frac{2\pi}{\lambda} \frac{1}{n_2} \sqrt{\sin^2 \alpha_1 n_1^2 - n_2^2} z\right]\end{aligned}$$

INTENSITY PROFILE

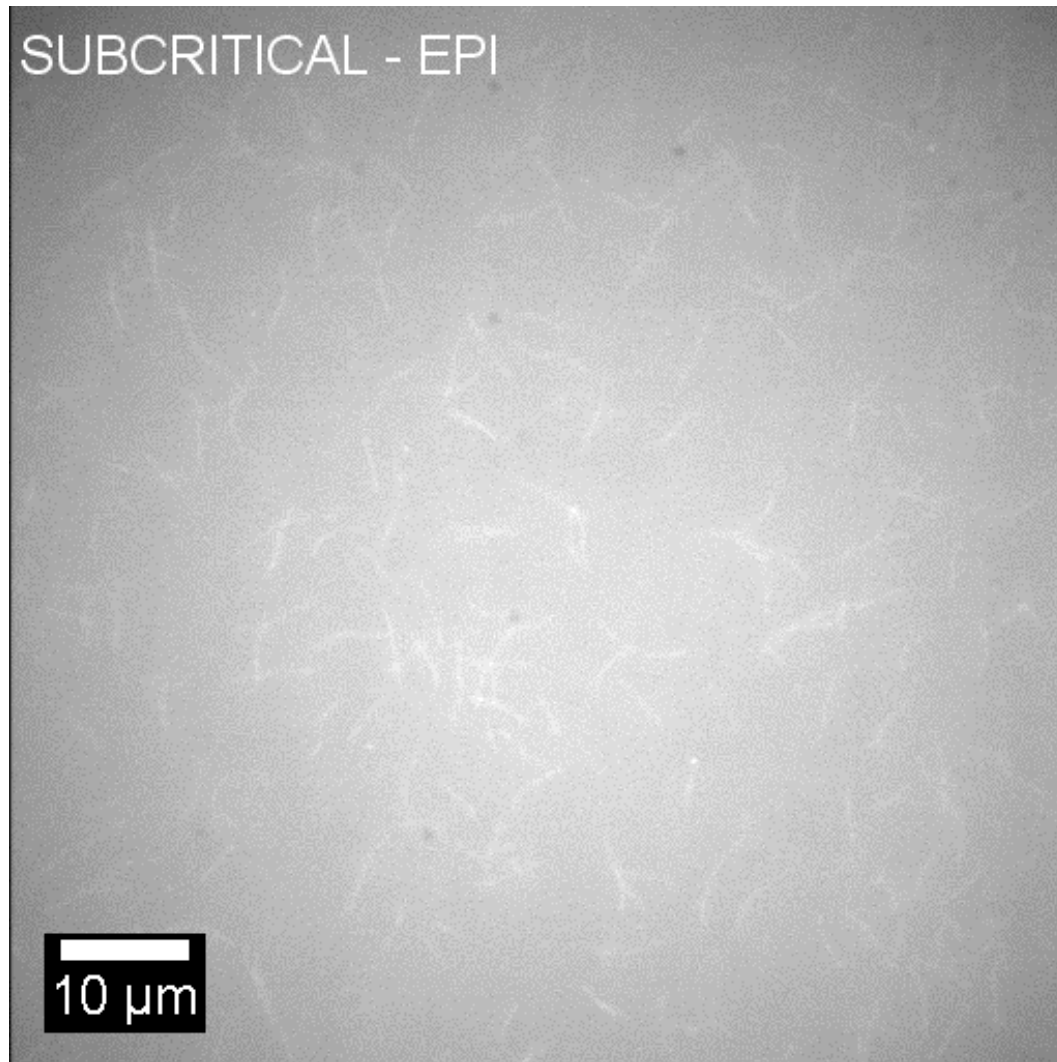
$$I(z) = |\vec{E}|^2 = I_0 \exp\left(-\frac{z}{d}\right)$$

PENETRATION DEPTH/DECAY LENGTH

$$d = \frac{\lambda}{4\pi n_1} \left(\sin^2 \alpha_1 - \left(\frac{n_2}{n_1}\right)^2\right)^{-\frac{1}{2}}$$



The decay length determines the axial resolution!
The shorter the decay length, the better the resolution.

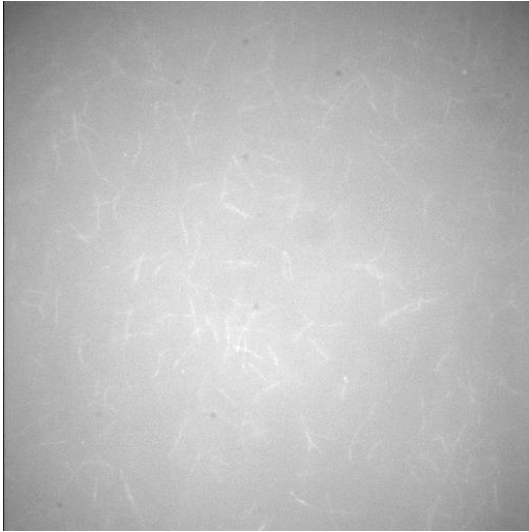


The onset of TIRF is obvious as a sudden darkening of the background and a flat 2D look to the features near the surface.

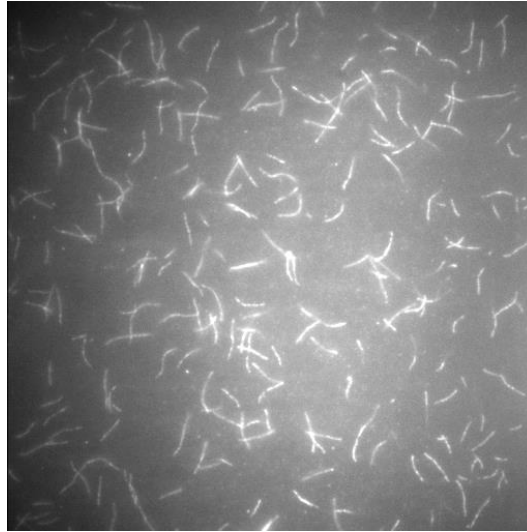
Alexa488NHS labeled actin filaments, Olympus IX81 inverted microscope, $\lambda_{\text{ex}} = 491 \text{ nm}$, 60× 1.49 NA

Wide-field vs TIRF illumination

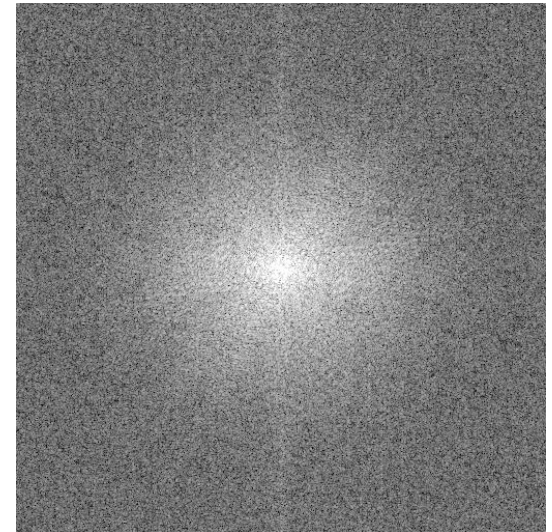
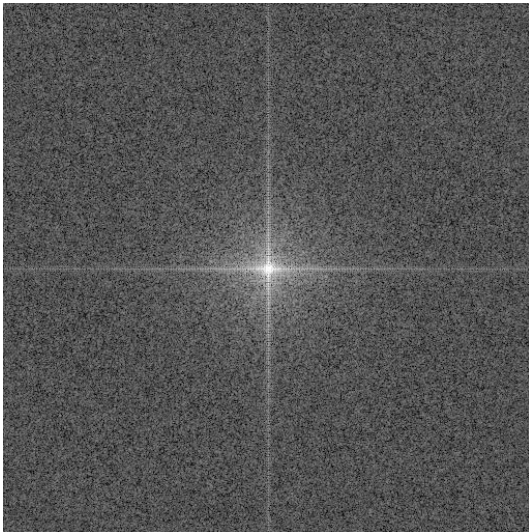
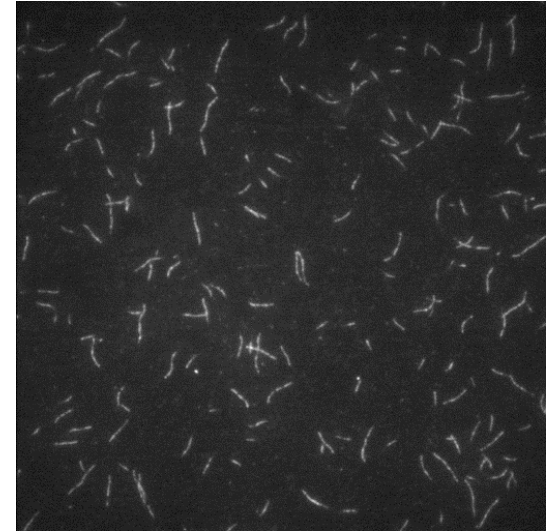
**Wide-field
subcritical angle**



critical angle

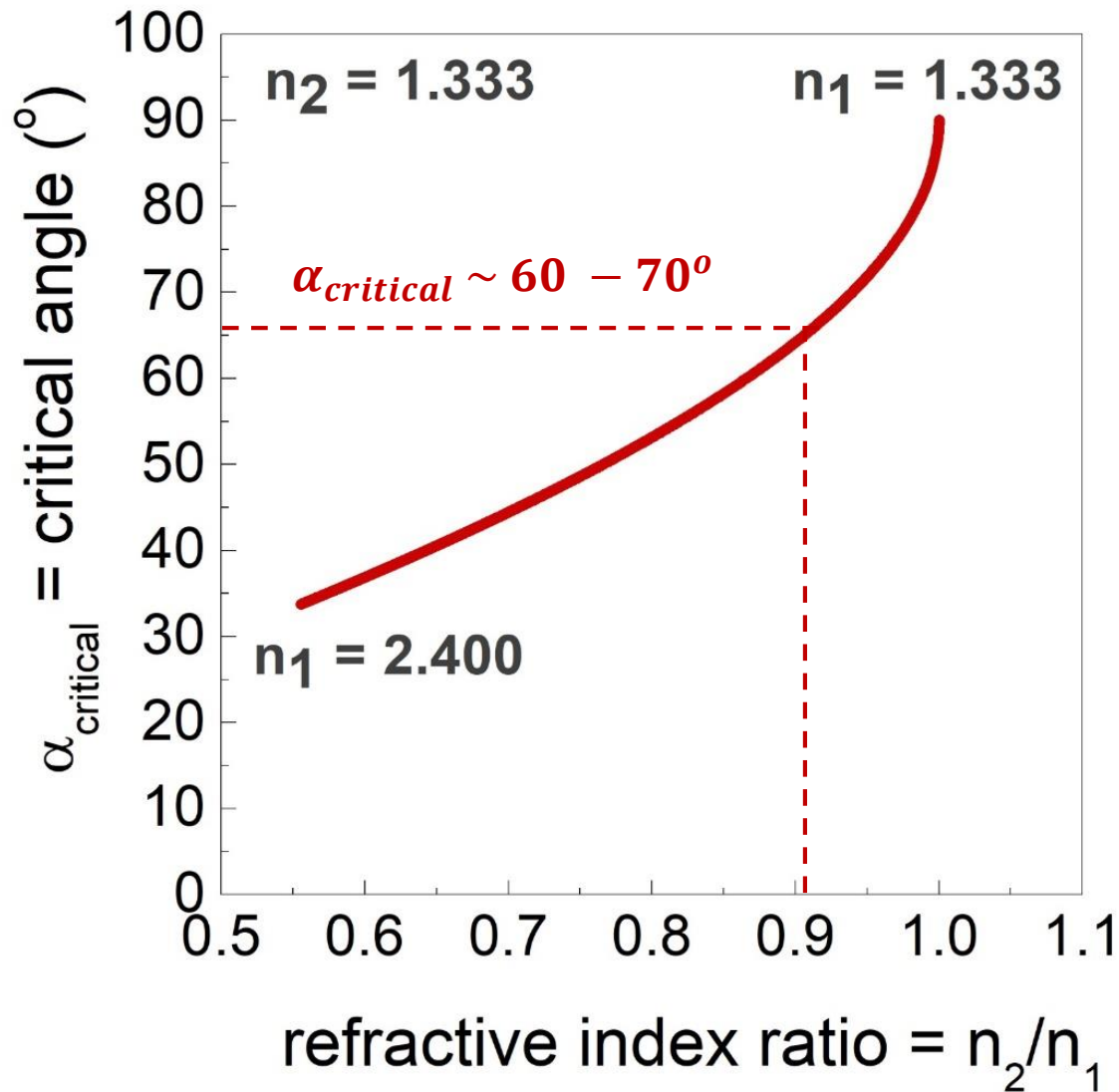


**TIRF
supercritical angle**



Total internal reflection – critical angle

$$\sin \alpha_{critical} = \frac{n_2}{n_1}$$



If $\frac{n_2}{n_1}$ is small, $\alpha_{critical}$ is shallow and TIR is easily achieved.

Influences on the resolution improvement

$$d = \frac{\lambda}{4\pi n_1} \left(\sin^2 \alpha_1 - \left(\frac{n_2}{n_1} \right)^2 \right)^{-\frac{1}{2}}$$

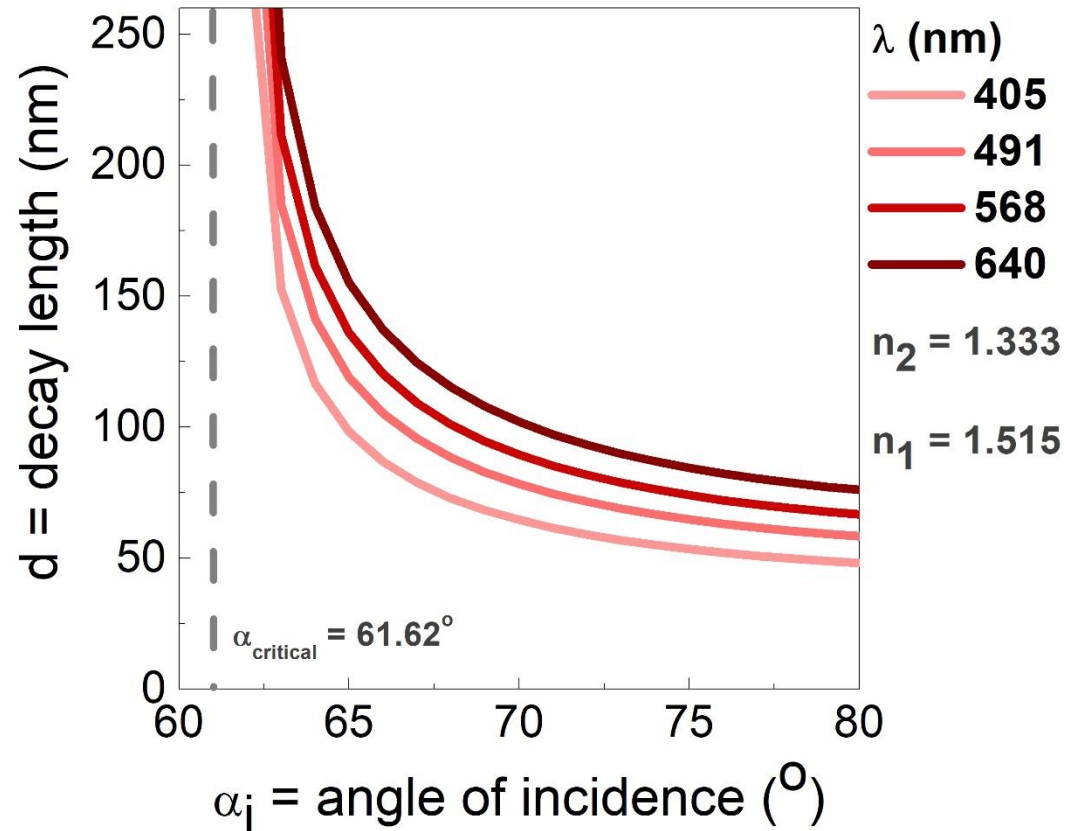
$$\lambda \downarrow \rightarrow d \downarrow$$

as the wavelength decreases, the depth is narrower.

$$\alpha_1 \uparrow \rightarrow d \downarrow$$

$$\alpha_1 \rightarrow \alpha_{\text{critical}}: d \rightarrow \infty$$

as the angle of incidence increases, the depth becomes narrower.



The shallower the evanescent field (smaller the d), the better the resolution.

The larger the angle of incidence, the better the resolution.

Influences on the resolution improvement

$$d = \frac{\lambda}{4\pi n_1} \left(\sin^2 \alpha_1 - \left(\frac{n_2}{n_1} \right)^2 \right)^{-\frac{1}{2}}$$

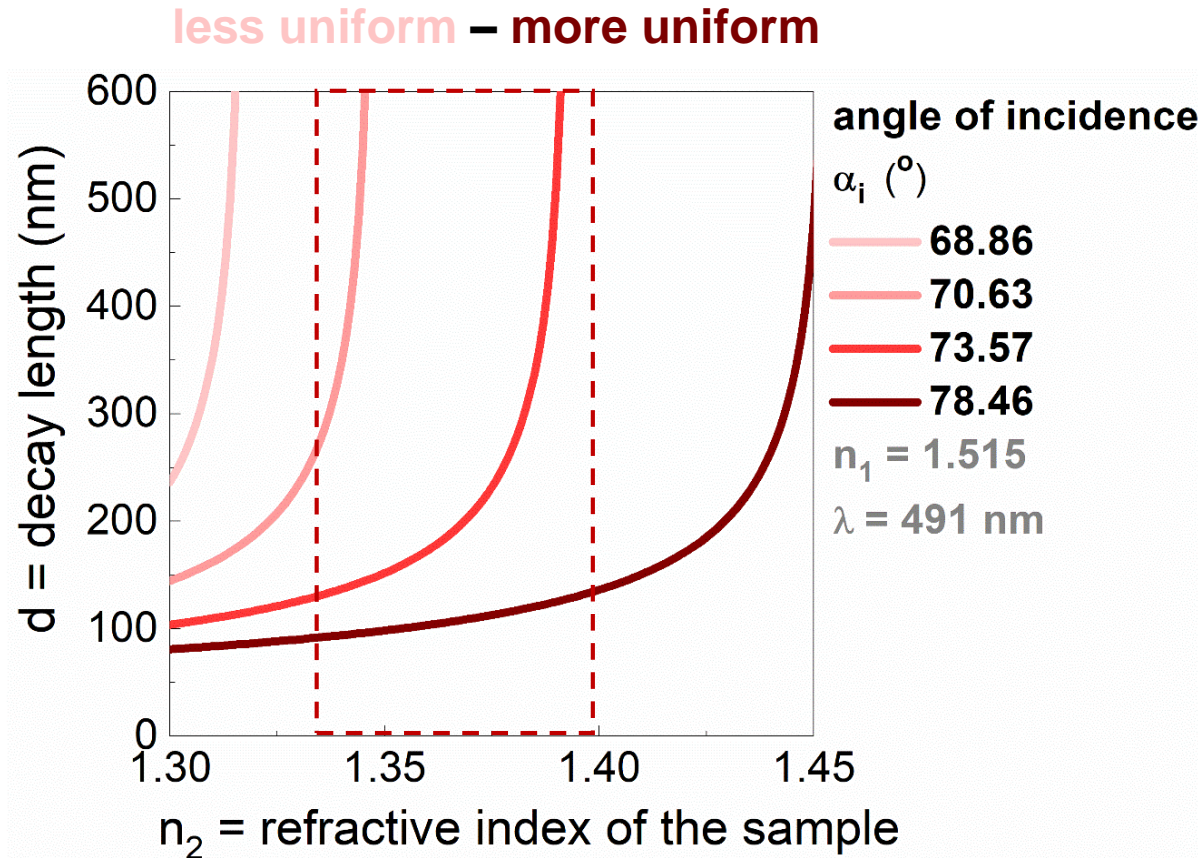
typical refractive index region of biological samples

$n_2 \uparrow \rightarrow d \uparrow$

as n_2 increases, the depth increases, which negatively influences resolution!

$\alpha_1 \uparrow \rightarrow$ sensitivity to $n_2 \downarrow$

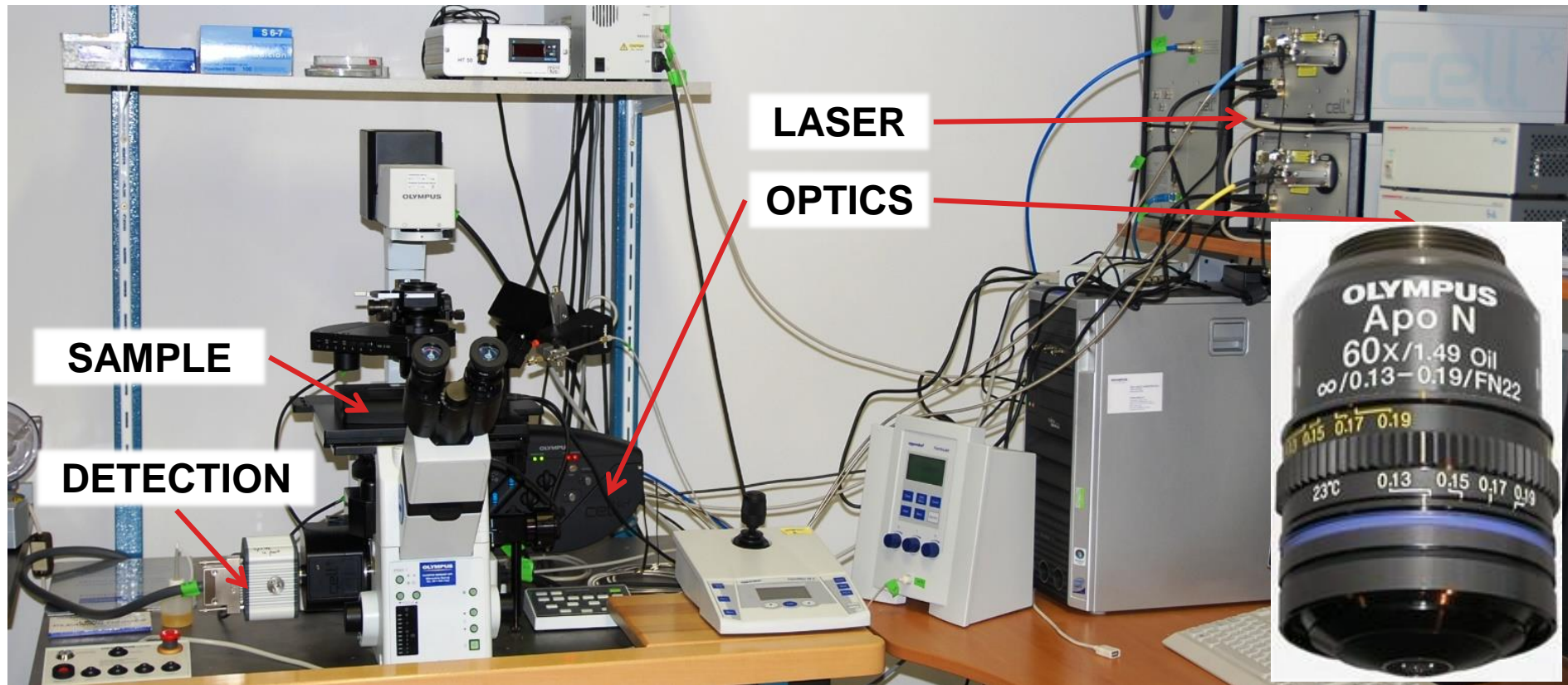
as the angle of incidence increases, the sensitivity of the evanescent field to n_2 decreases.



We do have refractive index inhomogeneity in the sample.

The larger the angle of incidence, the refractive index inhomogeneity of the sample has less influence on the decay length of the evanescent field, TIR illumination is more robust.

How to set up a TIRF microscope?



upgrade checklist:

- laser(s) for illumination
- special objective
- optics to couple, focus and adjust laser beam(s)

How to implement TIR principles into the fluorescence microscope?

▪ REFRACTIVE INDEX RATIO

THE REFRACTIVE INDEX OF THE 2ND MEDIUM HAS TO BE LOWER THAN THAT OF THE 1ST ONE

$$n_1 > n_2$$

$$n_{\text{coverglass}(1)} = 1.515$$

$$n_{\text{water}(2)} = 1.333 - n_{\text{cell}(2)} = 1.38$$

use of immersion medium ($n_{\text{oil}} = 1.515$) to provide continuous optical contact along the light path

▪ CRITICAL ANGLE OF ILLUMINATION

Limits resolution and the robustness of TIRFM!!

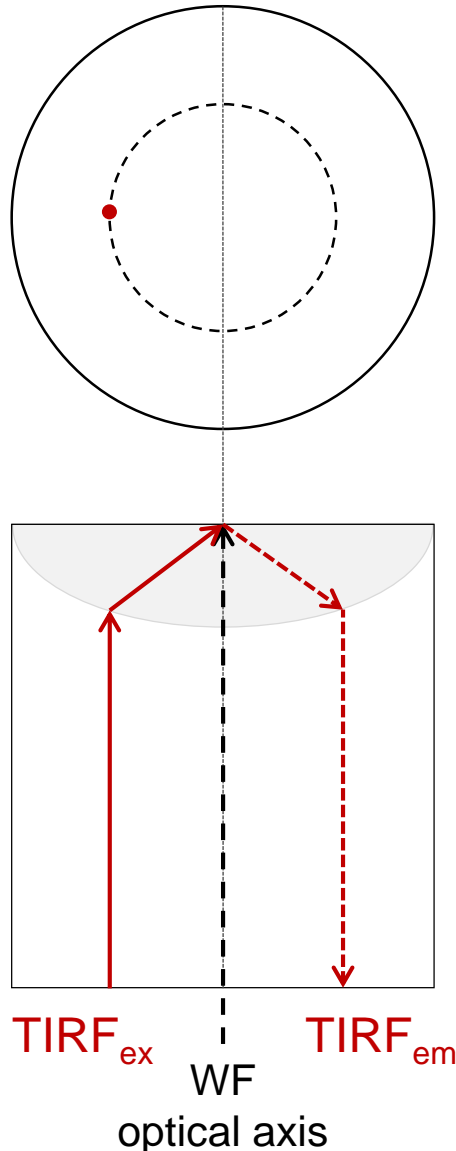
THE ANGLE OF INCIDENCE HAS TO BE LARGER THAN THE CRITICAL ANGLE

$$\alpha_{\text{incidence}} > \alpha_{\text{critical}}$$

$$\text{for glass : water interface: } \alpha_{\text{critical}} = 61.62^\circ$$

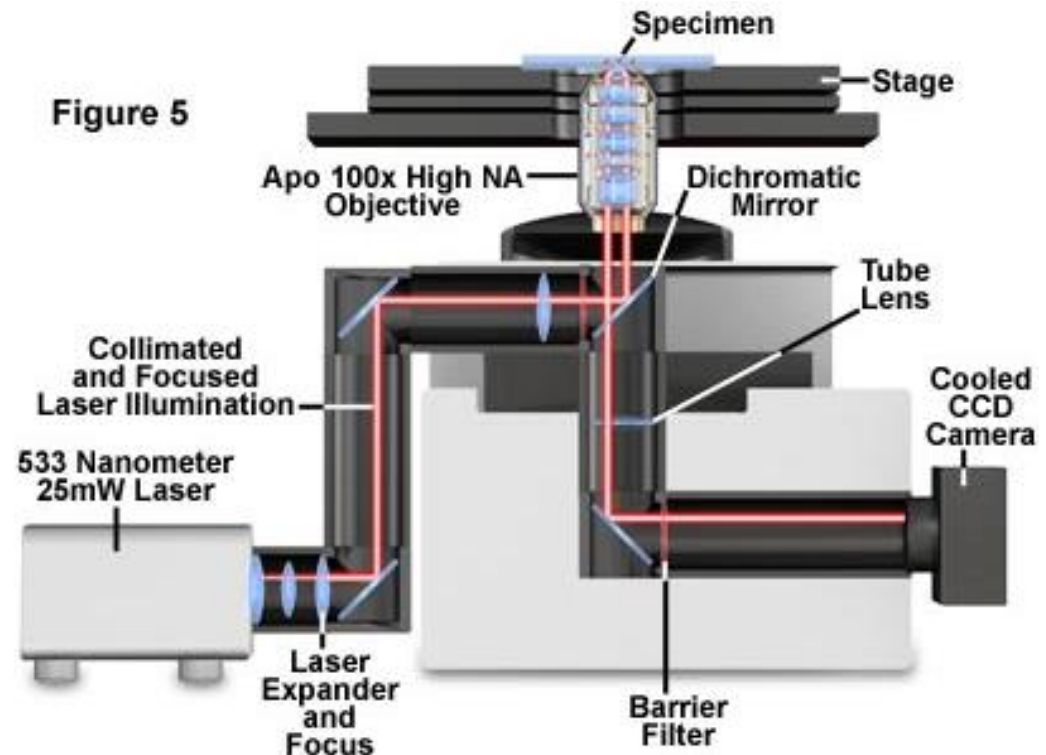
$$\text{for glass : cell interface: } \alpha_{\text{critical}} = 65.62^\circ$$

How to achieve the critical angle of illumination





Laser beam alignment

- in wide-field mode it is ,perfectly' aligned to the optical axis of the objective
- is focused in the back focal plane of the objective
collimated light; all the rays are parallel and all go at the same angle (all are totally internally reflected)
- in off axis position relative to the optical axis of the objective




Setting up laser-based illumination

Setup Parameters

Connectivity:  

Refract. Ind. Oil:









Refract. Ind. Sample:  <-- Current NA


Objective:

Critical Angle [°]:

Max Angle [°]:

TIRF Adjustment

Laser	Fiber Position [mm]	Penetration Depth [nm]
<input checked="" type="checkbox"/> 405 nm	 <input type="text" value="2.3075"/> 	<input type="text" value="100"/>
<input checked="" type="checkbox"/> 491 nm	 <input type="text" value="2.3450"/> 	<input type="text" value="101"/>
<input checked="" type="checkbox"/> 561 nm	 <input type="text" value="2.3775"/> 	<input type="text" value="100"/>
<input checked="" type="checkbox"/> 640 nm	 <input type="text" value="2.4150"/> 	<input type="text" value="100"/>



Fiber Positions:

Numerical aperture of the objective

glass : water interface

$$n_{\text{water}(2)} = 1.333$$

$$n_{\text{glass}(1)} = 1.515$$

$$n_{\text{immersion}(1)} = 1.515$$

$$\alpha_{\text{critical}} = 61.62^\circ$$

$$NA(\text{minimum}) = 1.515 \times \sin 61.62^\circ = 1.33$$

$$NA \sim 1.4$$

glass : cell interface

$$n_{\text{cell}(2)} = 1.38$$

$$n_{\text{glass}(1)} = 1.515$$

$$n_{\text{immersion}(1)} = 1.515$$

$$\alpha_{\text{critical}} = 65.62^\circ$$

$$NA(\text{minimum}) = 1.515 \times \sin 65.63^\circ = 1.38$$

$$NA > 1.4!$$



Numerical aperture of the objective

	WD (mm)	NA	n_1 immersion	n_2 cell	critical angle (°)	maximum angle (°)	utilized NA fraction
plan apochromatic	-	1.4	1.515	1.38	65.63	67.53	0.02
UAPON 150XTIRF	0.08	1.45	1.515	1.38	65.63	73.15	0.07
APON 60XTIRF UAPON 100XTIRF	0.1 0.1	1.49	1.515	1.38	65.63	79.57	0.11
APON 100XTIRF	0.08	1.65 *	1.788	1.38	50.51	67.34	0.27

* special immersion oil and glass coverslip are needed

The excitation light has to pass through the portion of the numerical aperture cone that is greater than ~ 1.4 .

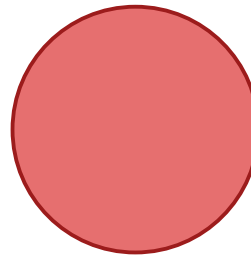
The larger the NA, the more flexibility you have, the more robust your TIRFM.

Being on the edge gives less flexibility.

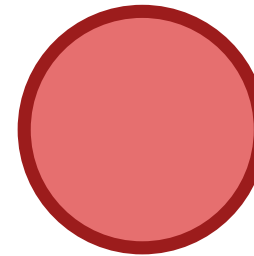
AVAILABLE NUMERICAL APERTURE MARGIN

minimum NA

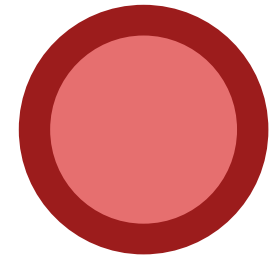
available NA



NA = 1.4
2 %

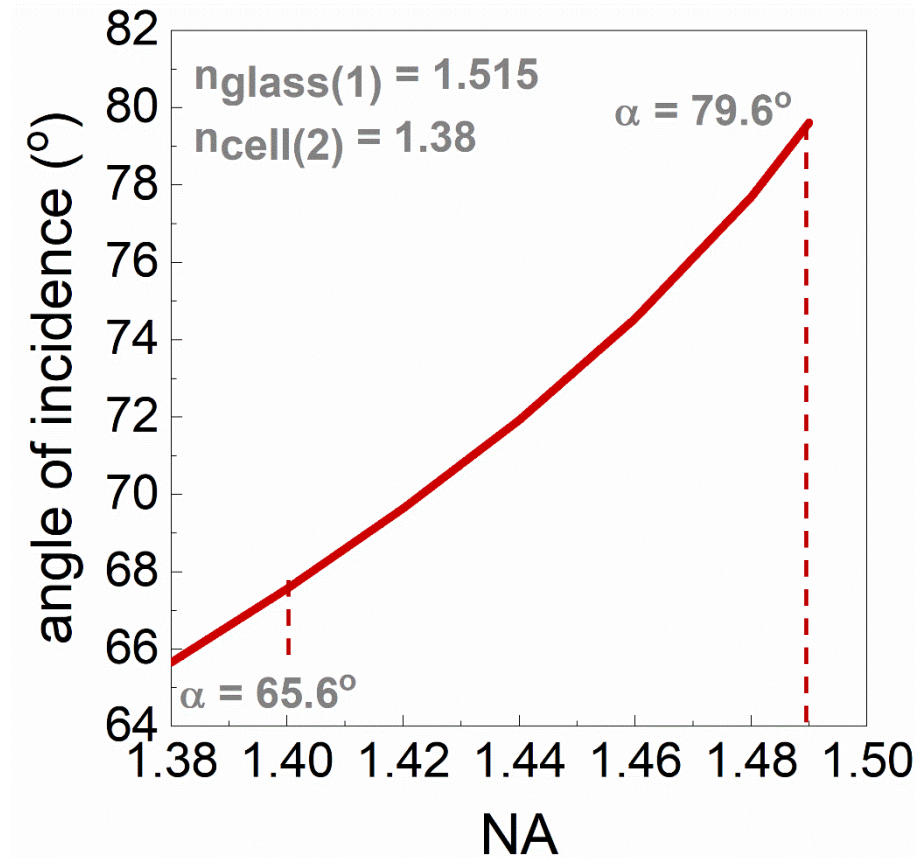
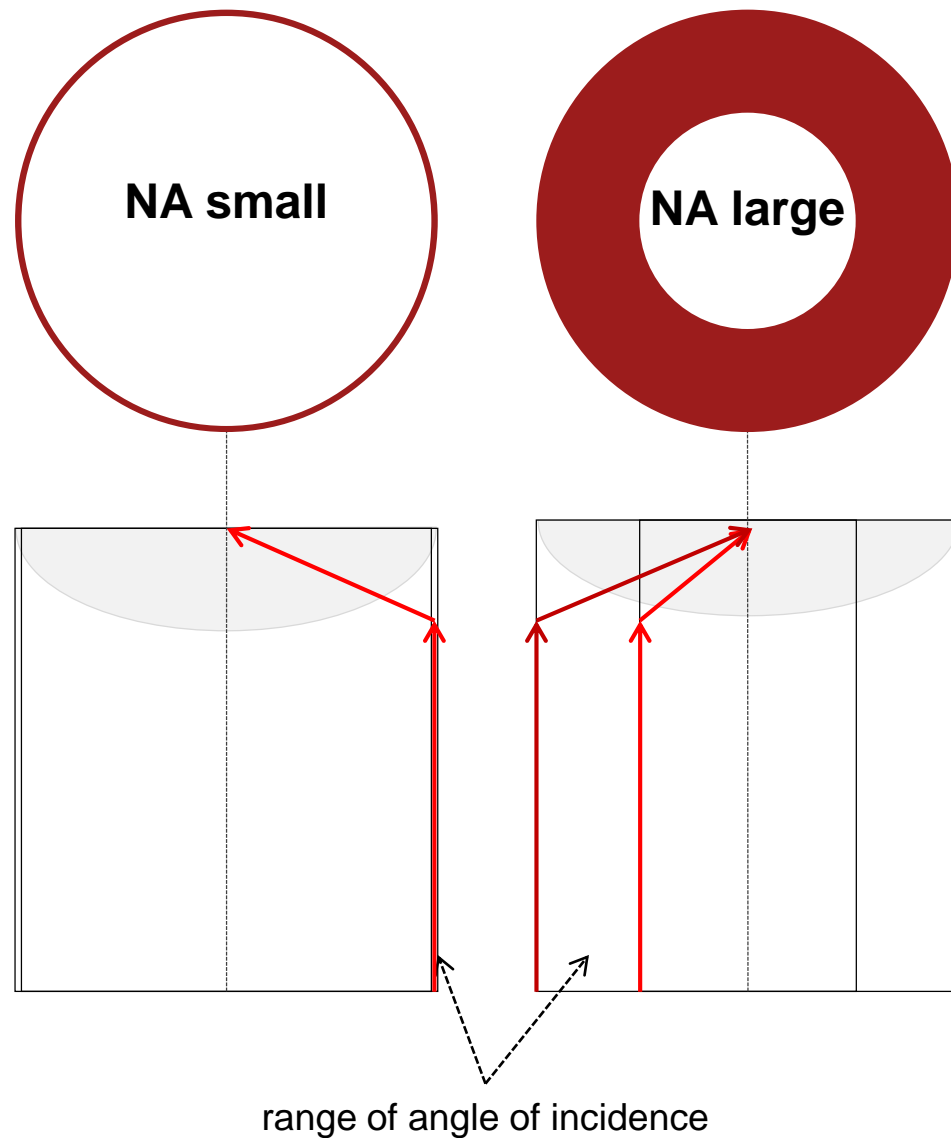


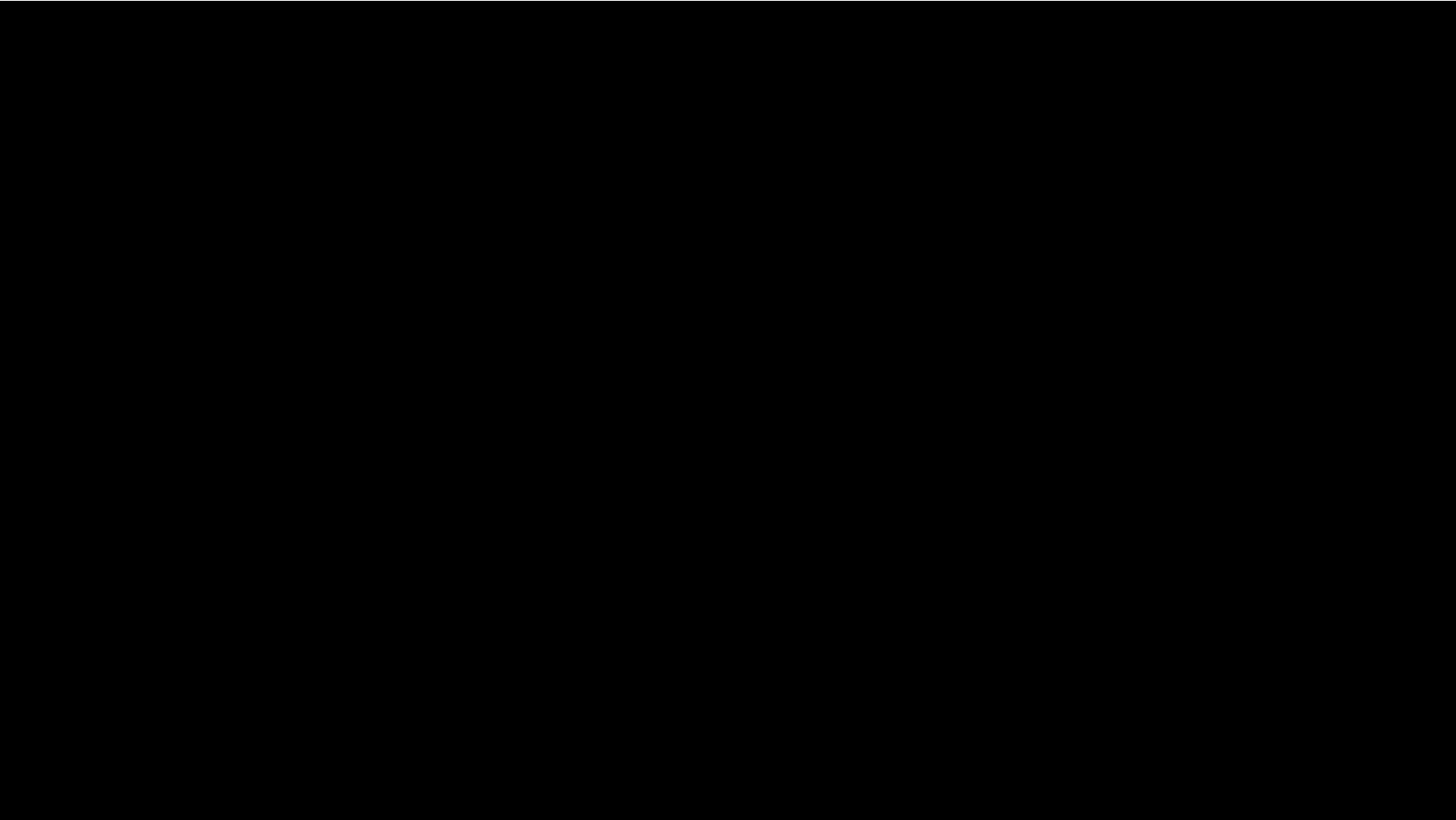
NA = 1.49
11 %



NA = 1.65
27 %

Numerical aperture of the objective





What TIRFM can/cannot do?

😊 😞 study structures/processes near/at a surface

- sample is either in focus or out-of-focus, it is not a question of where you focus
- TIRFM: single layer – confocal microscopy: any layer

→ 😊 **cylindrical lens, Z (axial) information**

😊 improved axial resolution $d_z \sim 100 \text{ nm}$

- depending on λ , n , NA

😞 classic lateral resolution $d_{x,y} \sim 200 \text{ nm}$

→ 😊 **TIRFM + SIM $d_{x,y} \sim 100 \text{ nm}$**

→ 😊 **TIRFM + STORM single molecule imaging $d_{x,y} \sim 10 \text{ nm}$**

😊 sample

- living/fixed cells adherent, recombinant proteins
- surface chemistry!
- coverslip, #1, 1.5!!
- no special need for sample preparation

😊 less cytotoxicity

- longer time-lapse movies

😊 does not require special fluorophore

😊 relatively easy to operate

😊 can be combined with other approaches

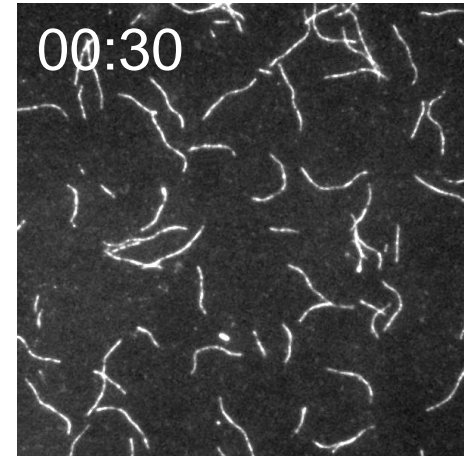
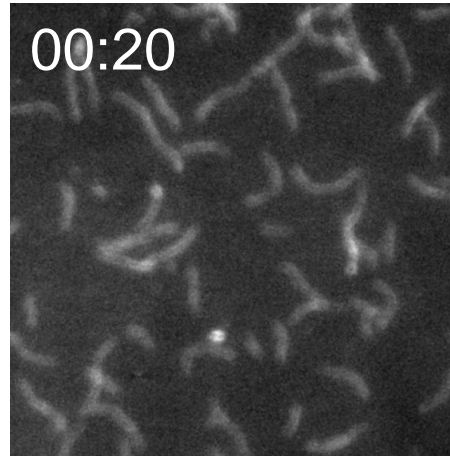
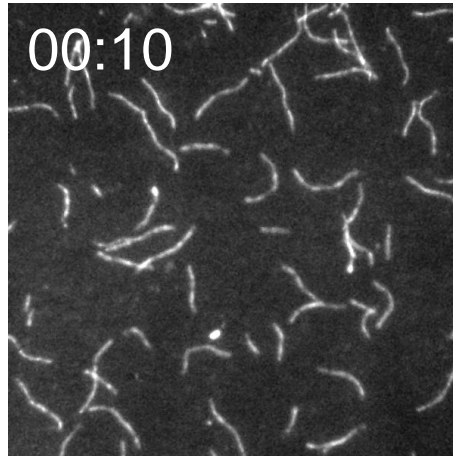
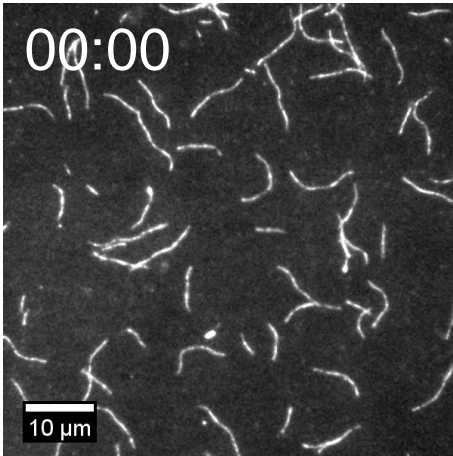
- FRAP, FRET, AFM, microfluidics, micropatterning

😞 irregular illumination field can degrade image quality

interference fringes, scattering, shadowing by cellular structures, improper alignment

→ 😊 **spinning TIRFM**

Troubleshooting – irregular illumination field



focus drifting

cause:

The thin optical section imaged with TIRF makes it **particularly sensitive to small changes in focus**, which degrade image quality.

solve:

- manually adjust focus
- focus-maintaining solution, Z drift compensator

Troubleshooting - irregular illumination field

below
supercritical regime

supercritical regime

contamination of image with propagating light

if the image can be focused in more than one z plane, then propagating light is a problem

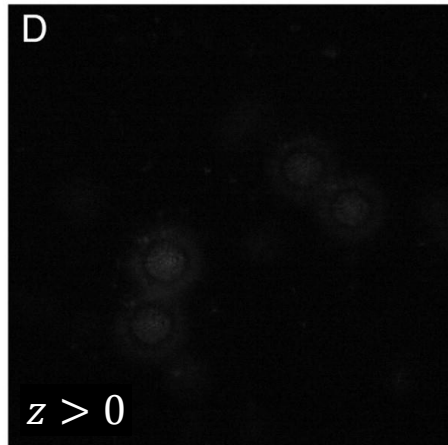
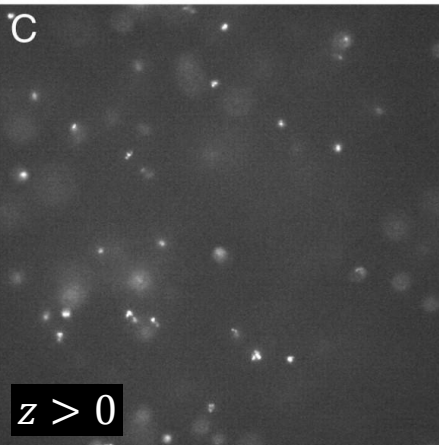
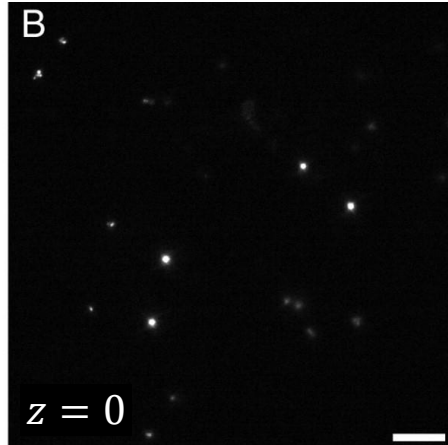
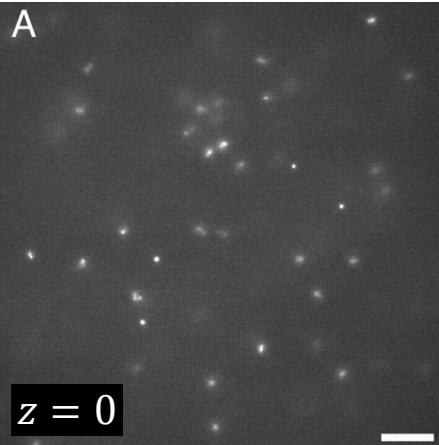
cause:

- improperly aligned laser (subcritical angle of incidence)
- tilted coverslip
- scattering by the sample

solve:

check the hardware; parameters of the TIRFM setup

- vary the incidence angle
- align laser



Troubleshooting - irregular illumination field

interference fringes

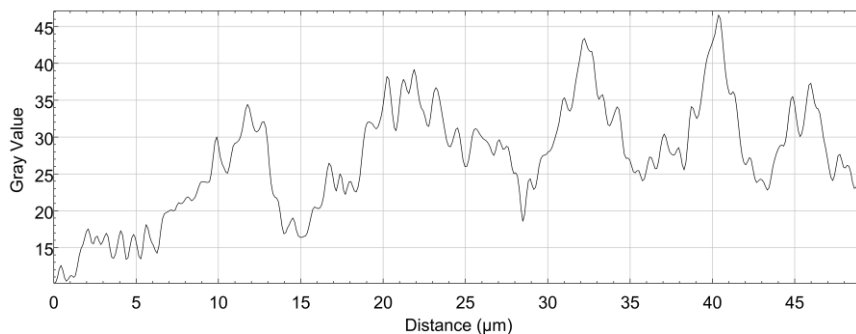
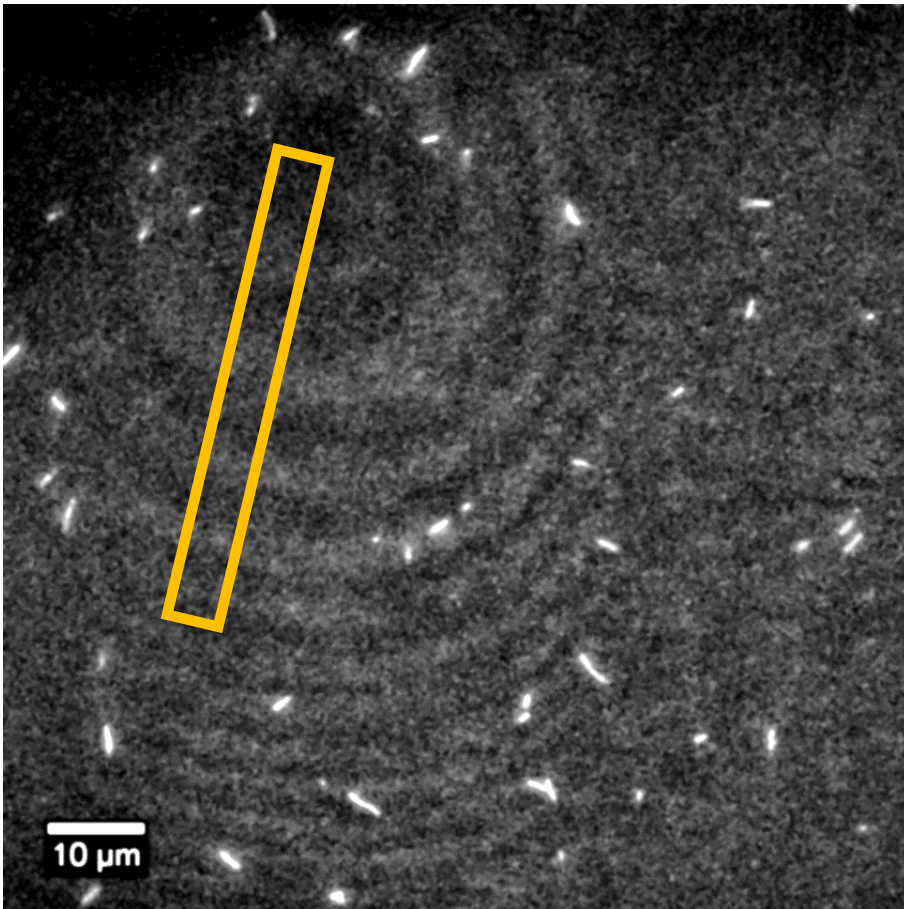
alternating light-dark pattern of excitation intensity at the sample plane is apparent

cause:

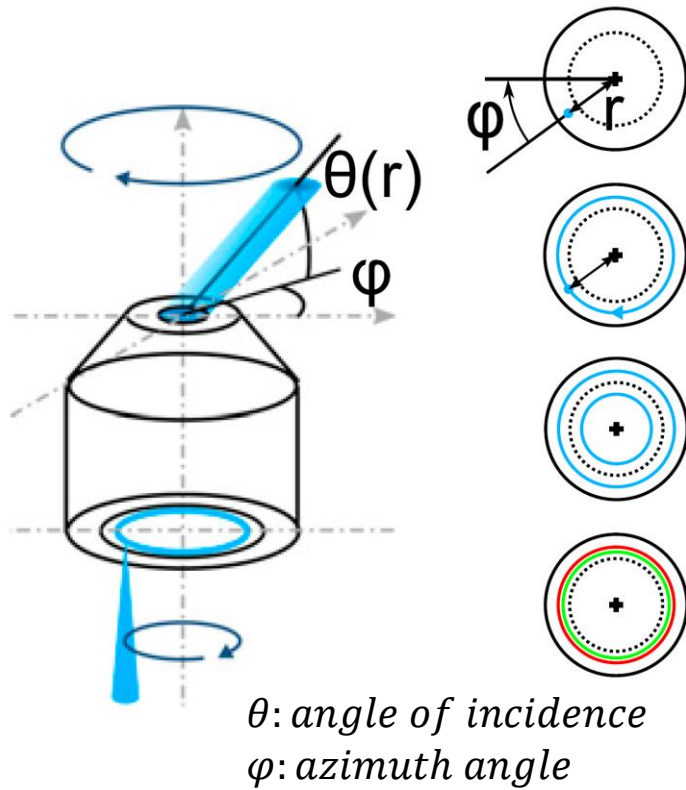
- optical imperfections in the beam path

solve:

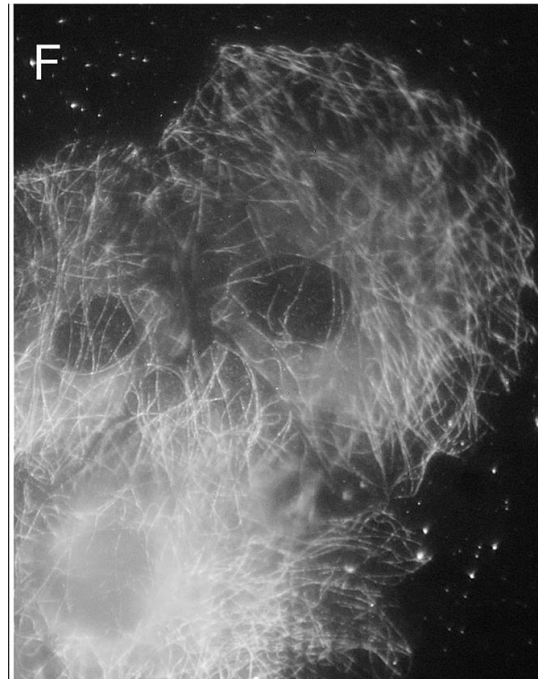
- cleaning dust off optical surfaces
- use dedicated optical elements
- spinning TIRFM



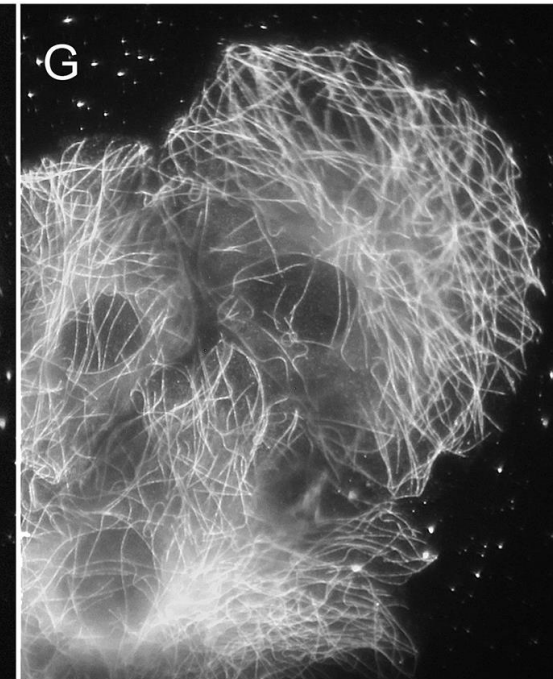
Troubleshooting: spinning TIRFM



stationary-spot TIRF



spinning-spot TIRF



(F-G) COS-7 cells expressing tubulin (EGFP), stationary-spot TIRF (F), spinning-spot TIRF (G).

Utilizes a pair of galvanometer mirrors to **spin the laser spot around a circle at the outer edge of the objective's back focal plane**. Consequently, a collimated beam with fixed polar angle and spinning azimuthal angle illuminates the specimen. The **different shadowing and interference patterns at each angle thus average out during the single-frame exposure time of the camera to produce a substantially uniform illumination field**.

Irregularities in the illumination field averages out.

TIRFM – cell biological applications

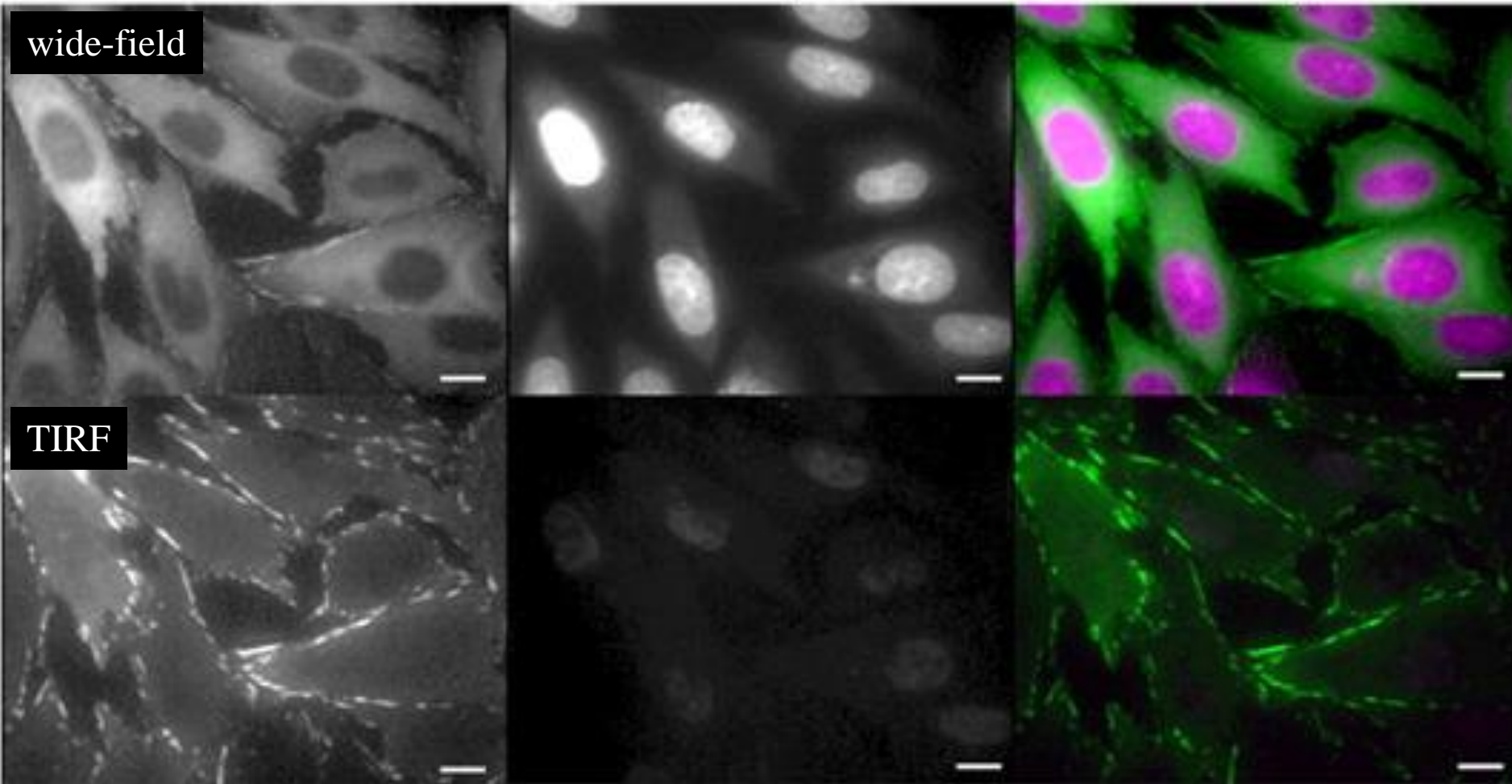
Paxillin-EGFP

Draq5

Overlay

wide-field

TIRF



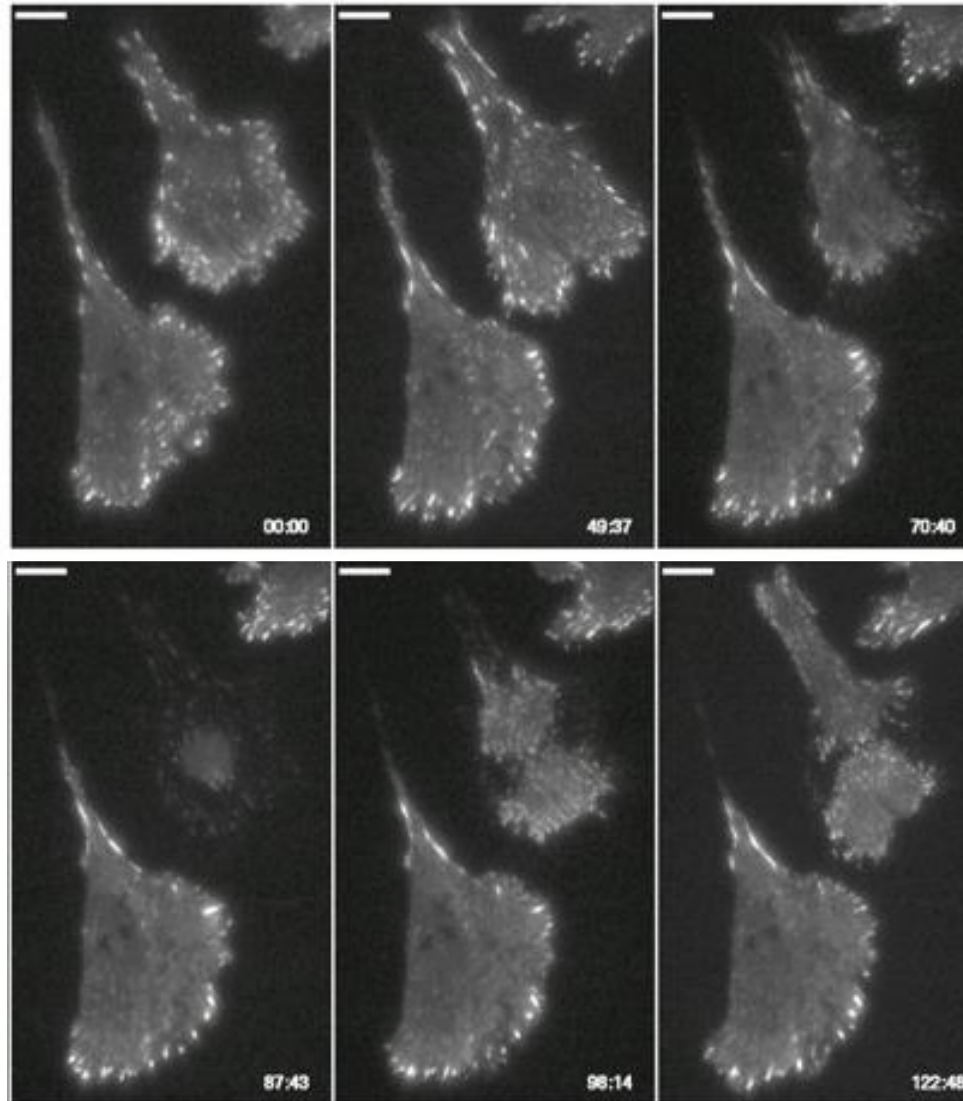
Chinese hamster ovary (CHO) cells, EGFP-paxillin. Scale bars: 10 μm .

PAXILLIN: focal adhesions, cell adherence to extracellular matrix

Draq5: Deep Red Anthraquinone 5, nucleic acid staining

Lack of nuclear/cytoplasmic staining – specificity for the basal cell surface.

TIRFM – cell biological applications

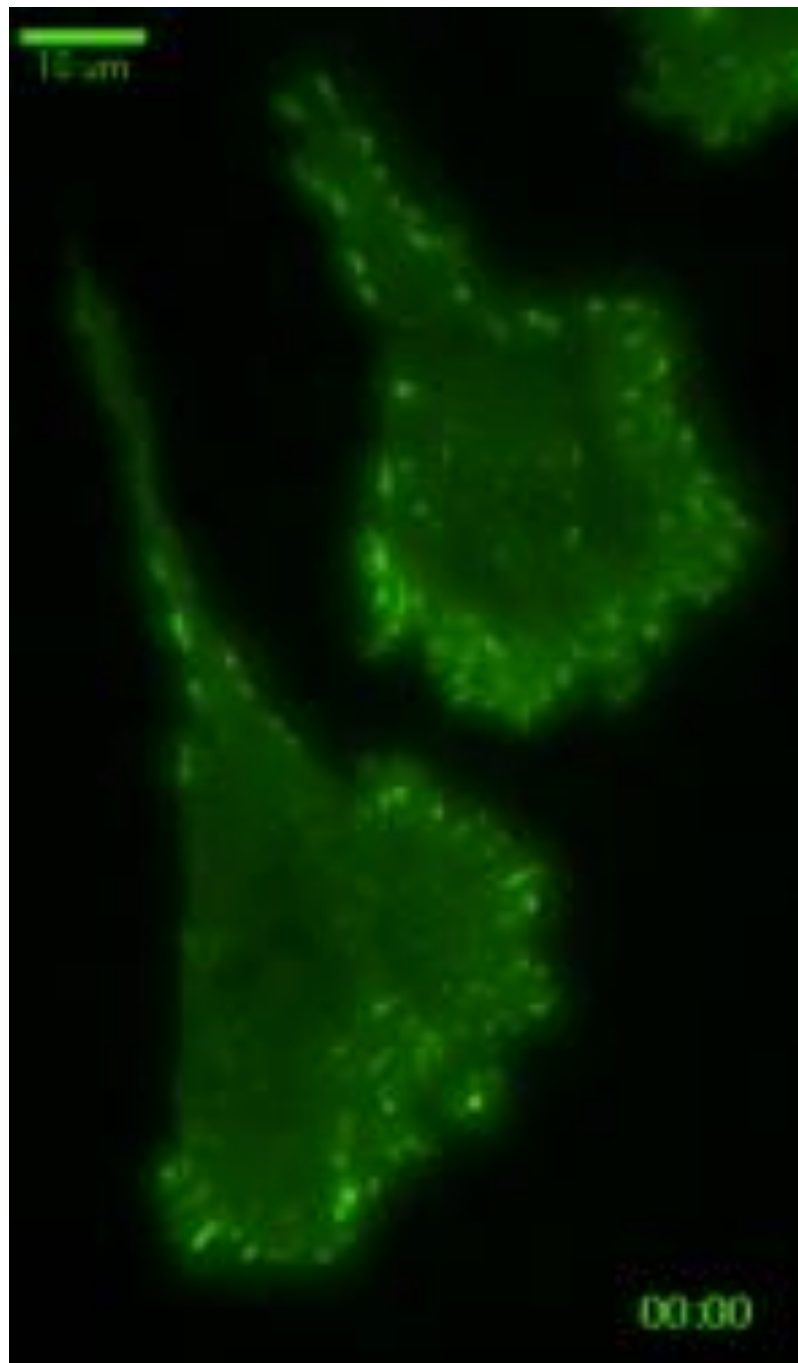


TIRF images of Chinese hamster ovary (CHO) cells, EGFP-paxillin. Scale bars: 10 μ m.

PAXILLIN: focal adhesions, cell adherence to extracellular matrix

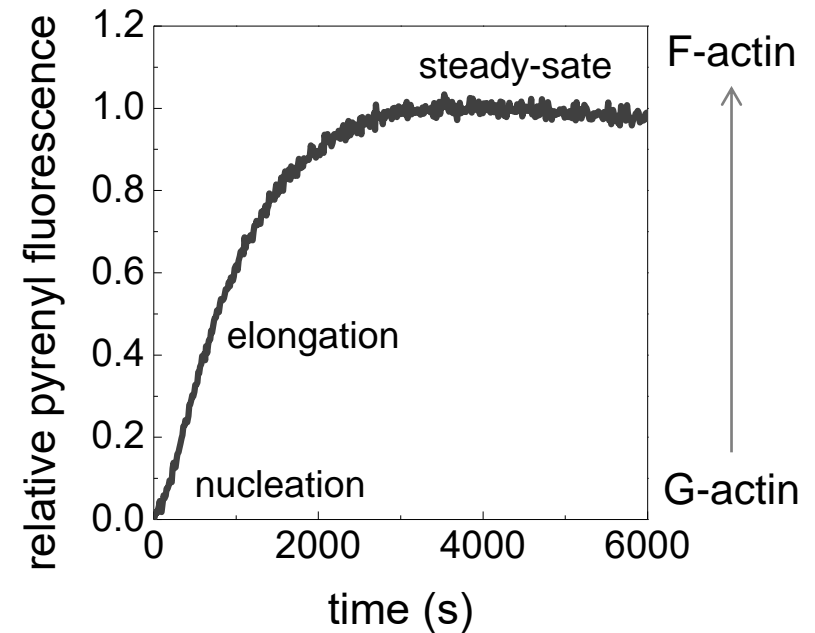
A cell rounds up and disappears from the TIRF field during cell division.

M. M. Frigault, J. Lacoste, J. L. Swift, C. M. Brown *Live-cell microscopy – tips and tools*. Journal of Cell Science 2009 122: 753-767; doi: 10.1242/jcs.033837



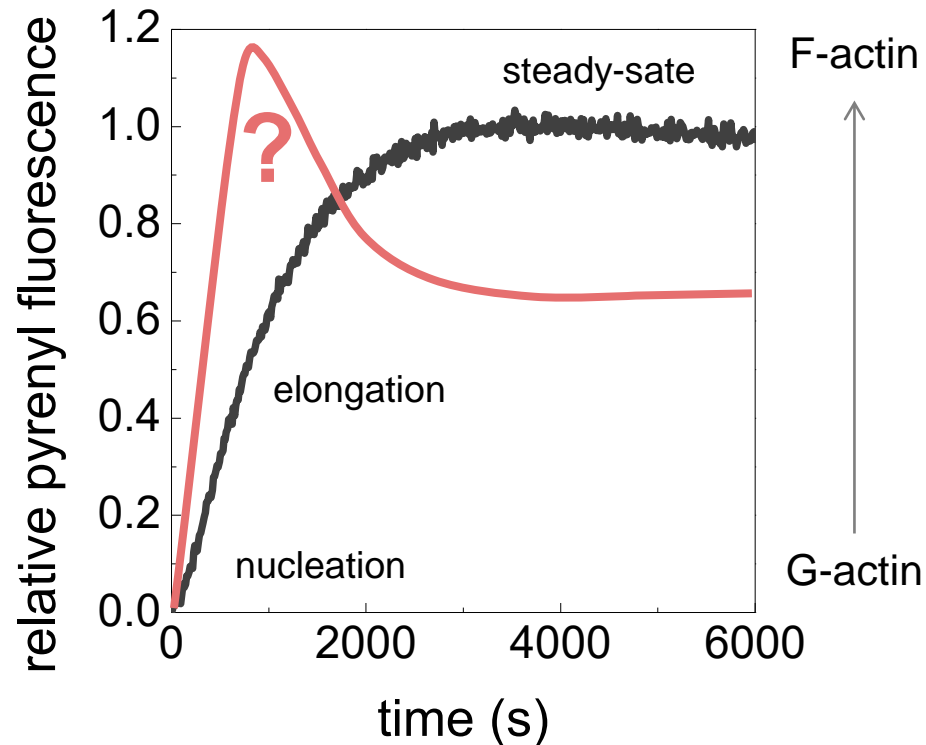
POLYMER BIOCHEMISTRY – ACTIN, MICROTUBULE DYNAMICS

SPONTANEOUS ACTIN ASSEMBLY



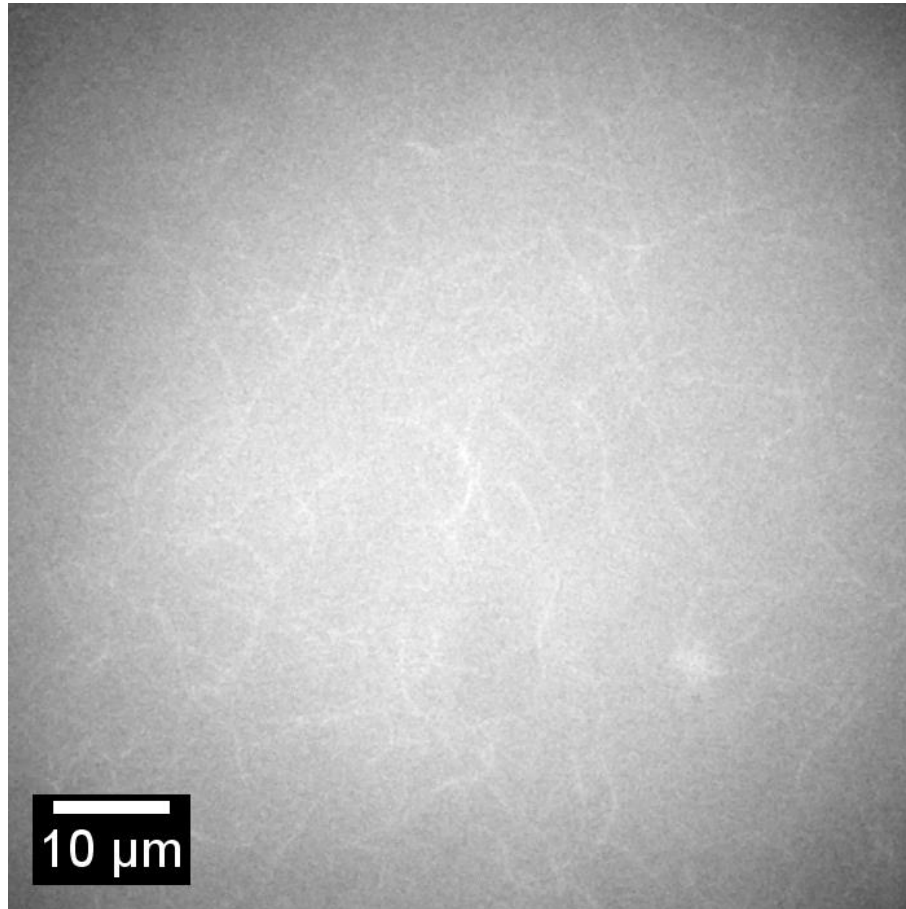
$$v = k_+[G_0 - c_c][F] - k_-[F]$$

SPONTANEOUS ACTIN ASSEMBLY

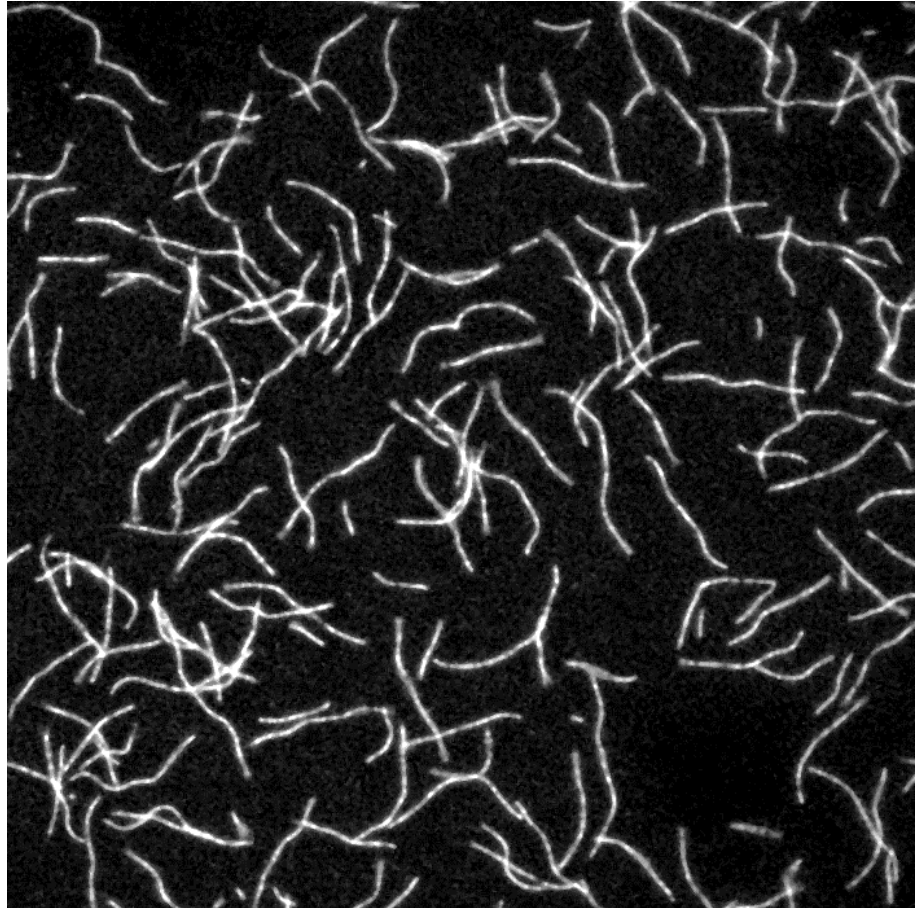


$$v = k_+[G_0 - c_c][F] - k_-[F]$$

Epi



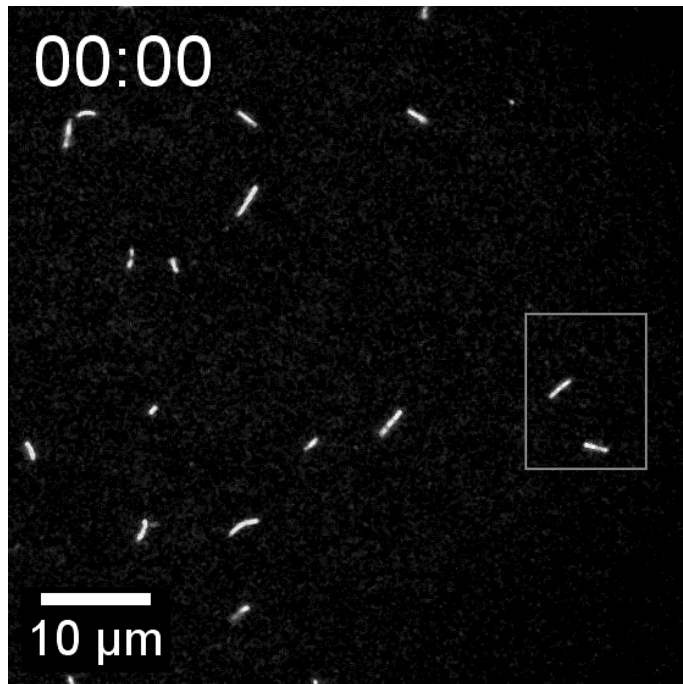
TIRF



Actin polymers - microfilaments in vitro (488 nm)

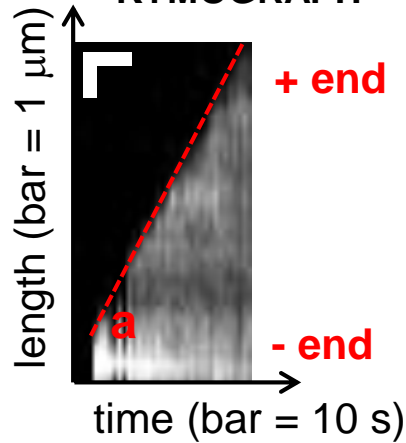
POLYMER BIOCHEMISTRY – ACTIN, MICROTUBULE DYNAMICS

SPONTANEOUS GROWTH OF ACTIN FILAMENTS



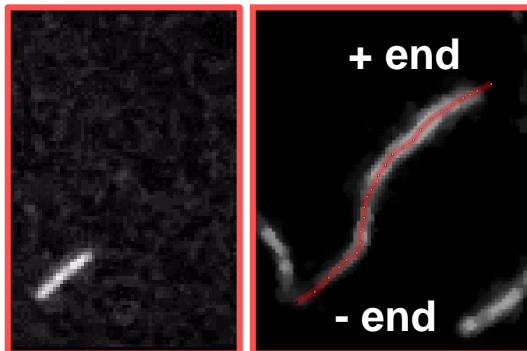
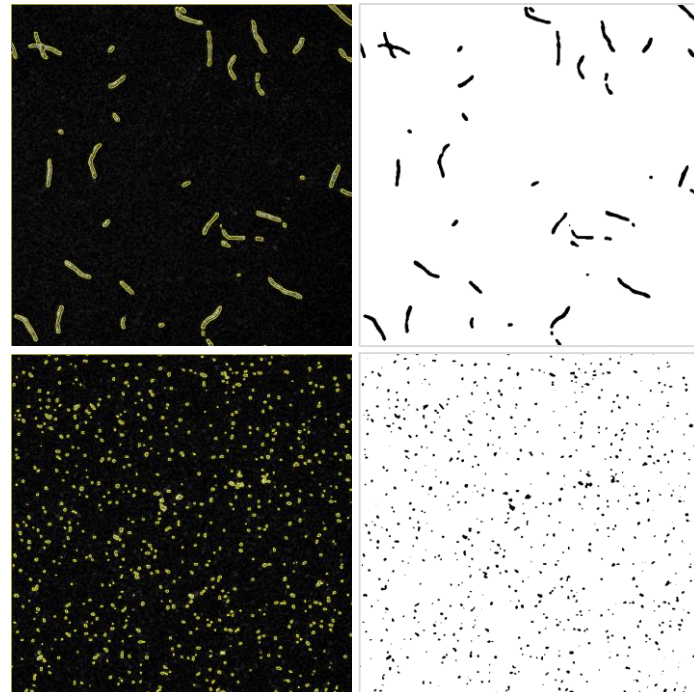
AlexaNHS488-ACTIN (10 % LABELED)
 491 nm 60xNA1.45 time = min : s
 t = 100 ms, I = 10% (P = 15 mW) HamamatsuCCD

KYMOGRAPH



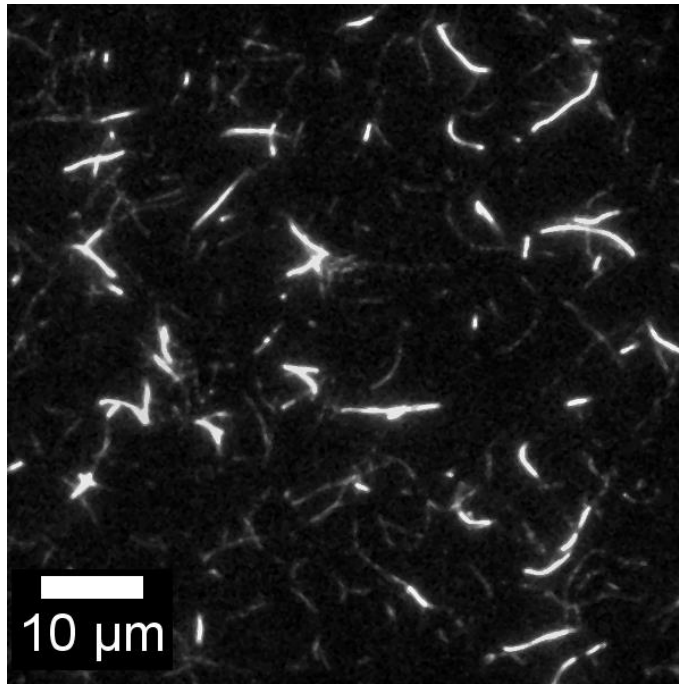
$$v_{\text{elongation}} = \tan \alpha = \frac{\Delta \text{length}(\mu\text{m})}{\Delta \text{time}(\text{s})} = \frac{\Delta \text{length} * 370(\text{su})}{\Delta \text{time}(\text{s})}$$

$$v_{\text{elongation}} = k_+[G - c_c] \rightarrow k_+ = 11 \mu\text{M}^{-1}\text{s}^{-1}$$



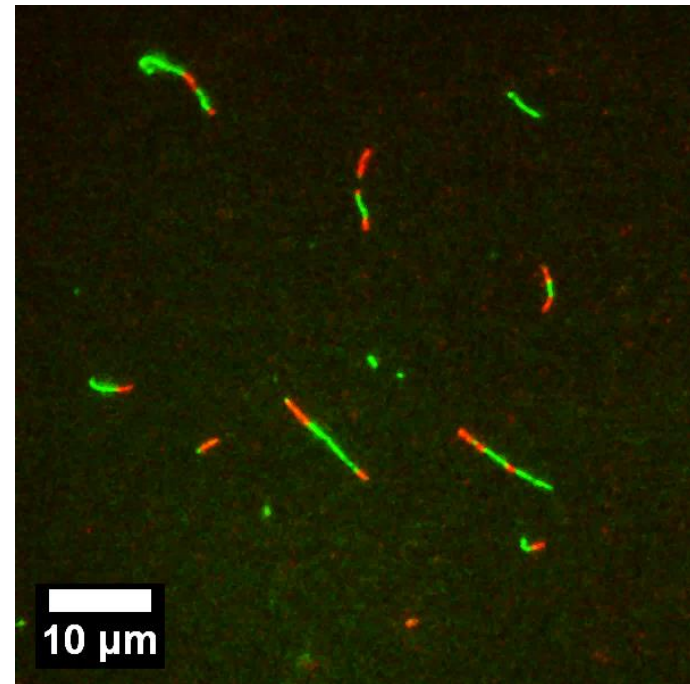
SPONTANEOUS ASSOCIATION OF INDIVIDUAL POLYMERS INTO HIGHER ORDER STRUCTURES

SIDewise ASSOCIATION cross-linking/bundling



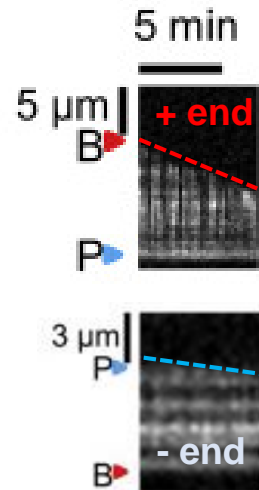
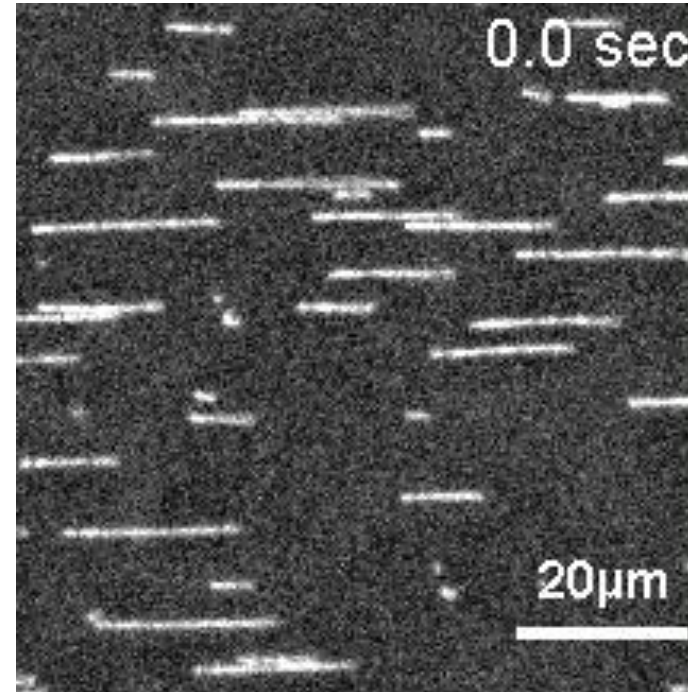
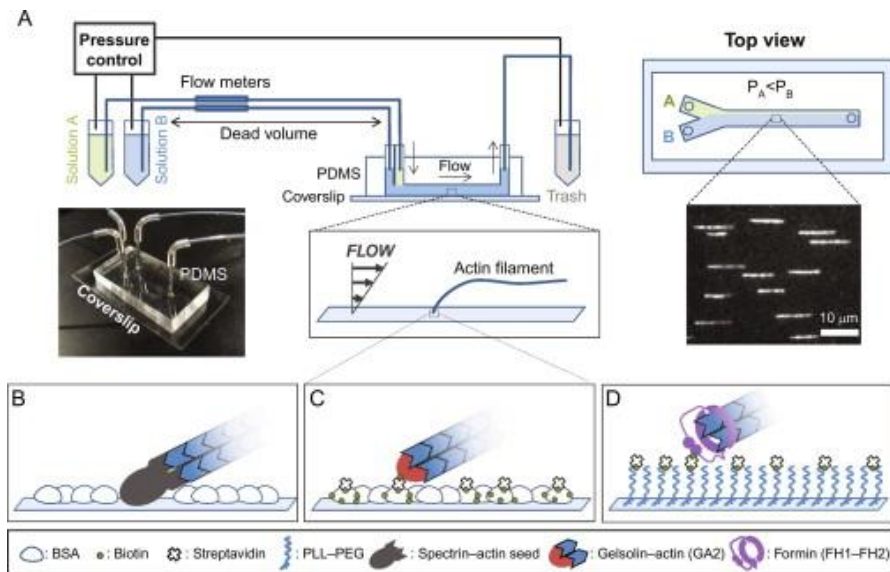
radial thickening

ENDwise ASSOCIATION annealing



lateral growth

SPONTANEOUS **DEPOLYMERIZATION** DISSOCIATION OF INDIVIDUAL SUBUNITS FROM POLYMER ENDS



MICROFLUIDICS-ASSISTED TIRF
OBSERVATION OF THE DISASSEMBLY OF
INDIVIDUAL ACTIN POLYMERS

$$k_{OFF}(\text{barbed end, ATP}) = 1.4 \text{ s}^{-1}$$

$$k_{OFF}(\text{pointed end, ADP}) = 0.25 \text{ s}^{-1}$$

TIRFM – cell biological applications

Glucose uptake

10 % adipose tissue, 90 % muscle

insulin resistance, type2 diabetes

translocation

plasma membrane

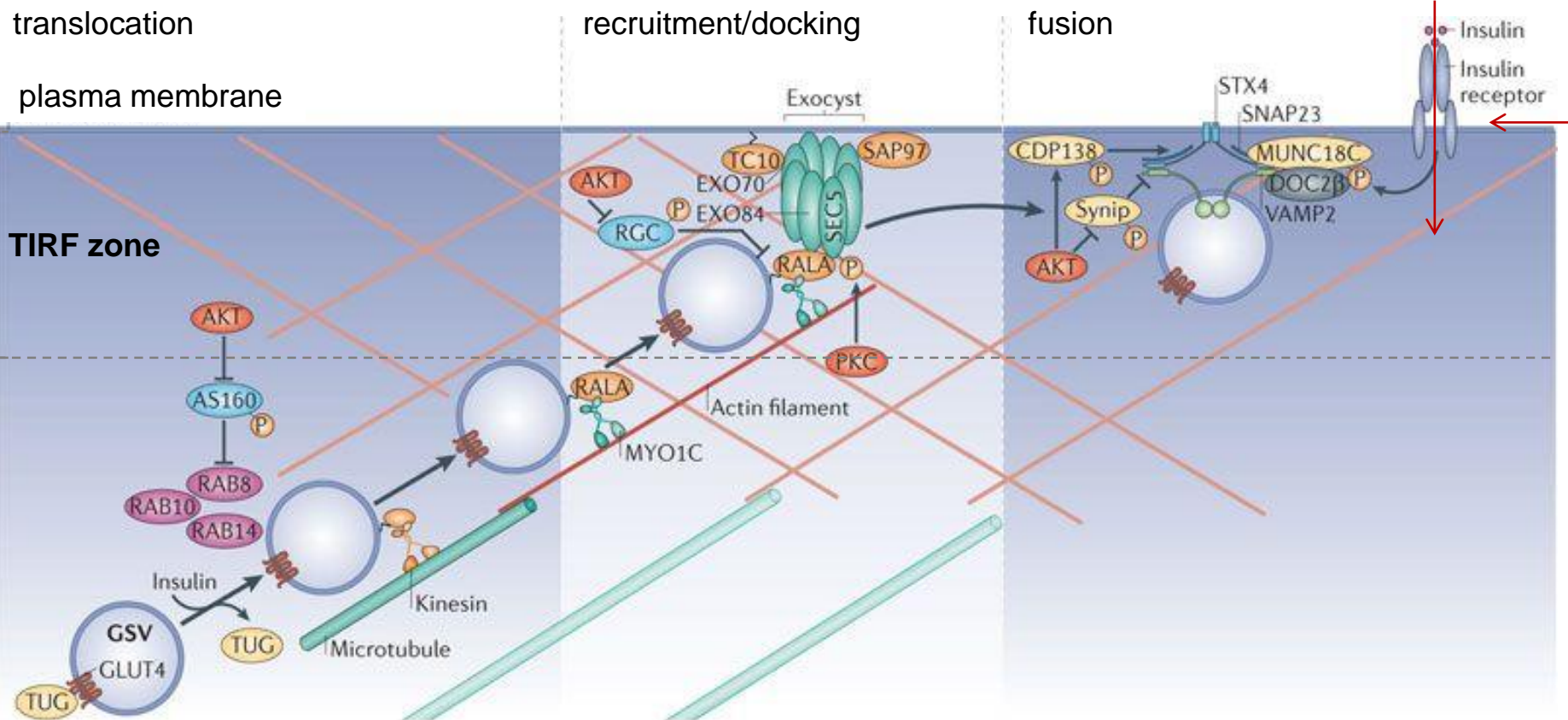
TIRF zone

recruitment/docking

fusion

insulin

glucose

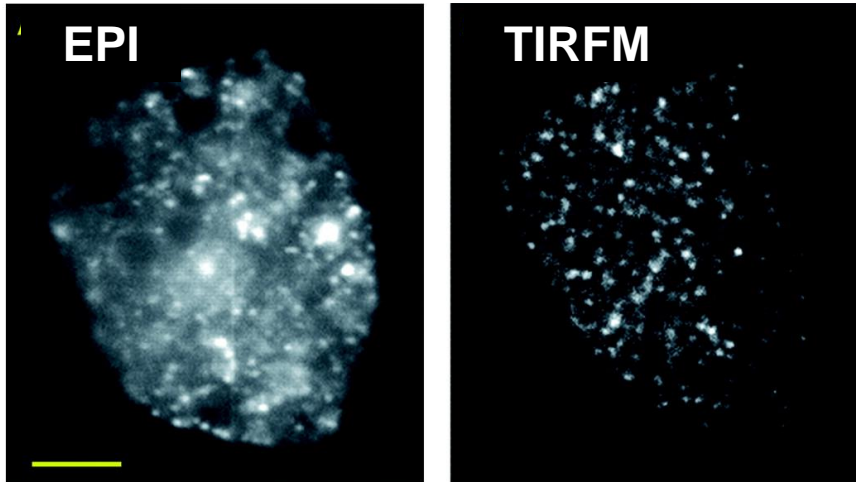


glucose transporter (GLUT4)

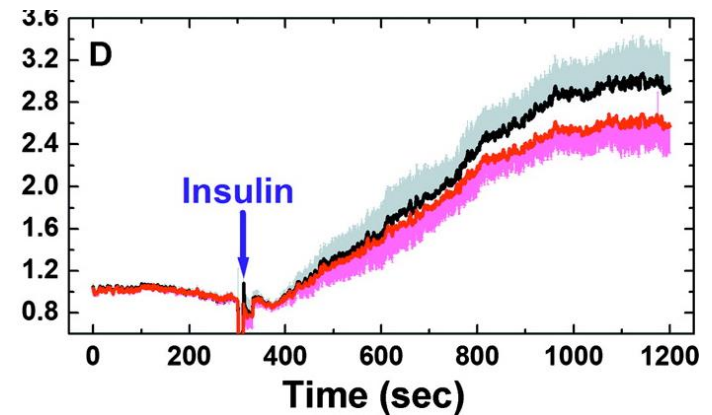
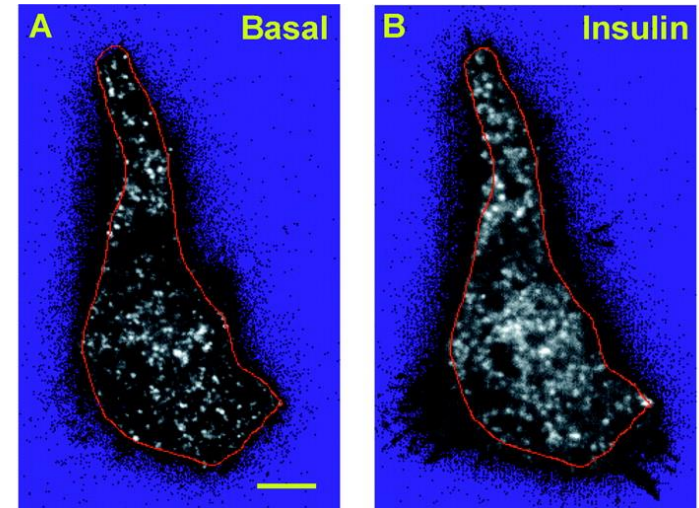
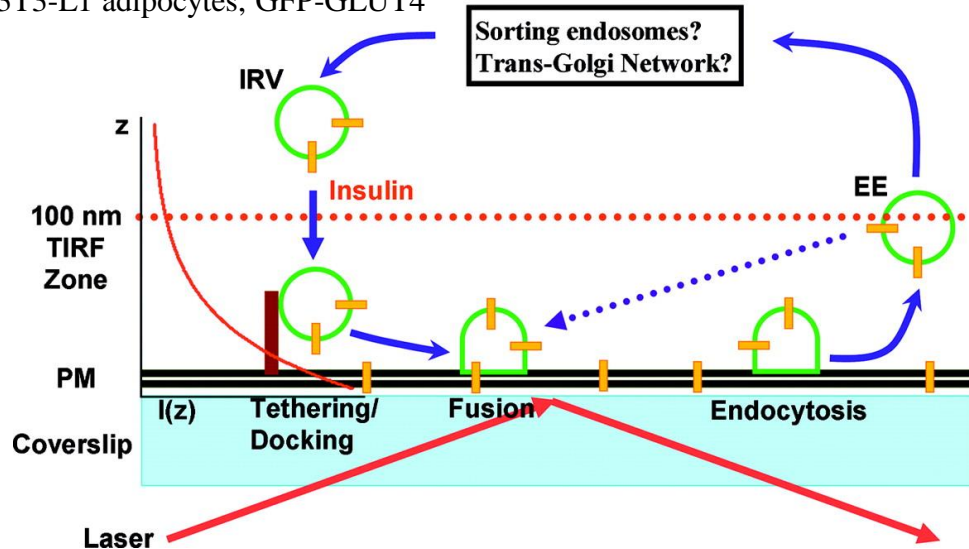
intracellular storage sites

TIRFM – cell biological applications

TIRFM: GLUT4 vesicles near or at the plasma membrane



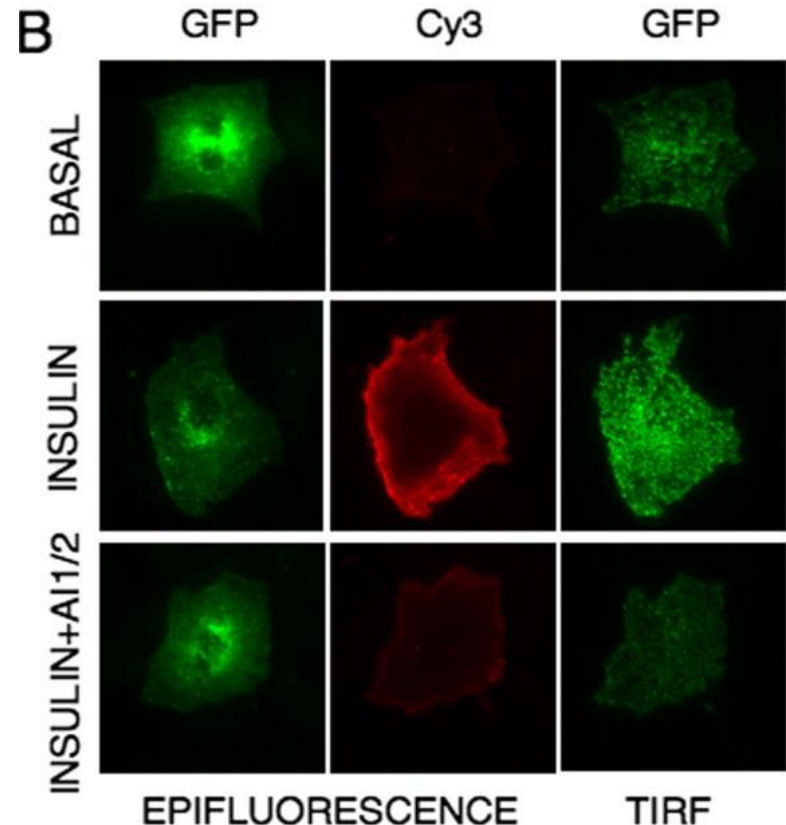
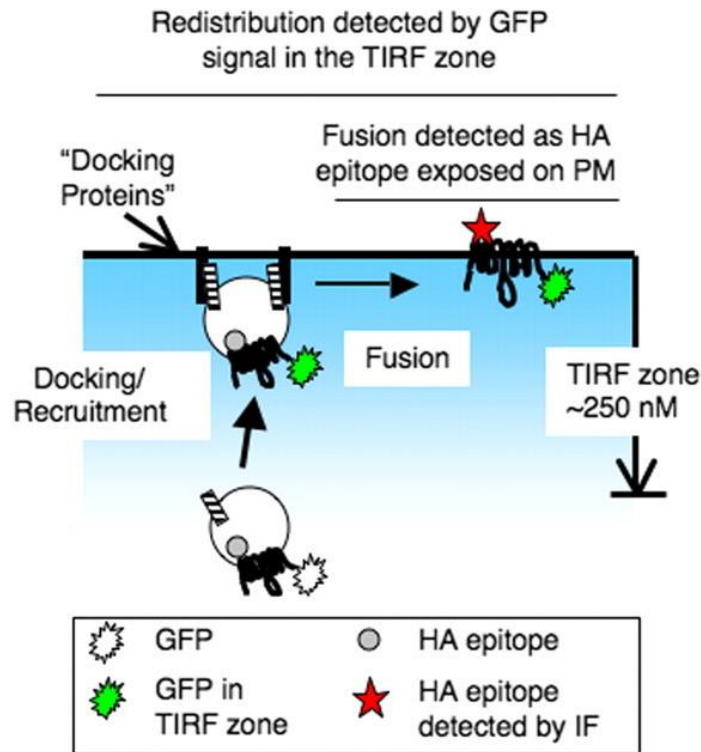
3T3-L1 adipocytes, GFP-GLUT4



TIRFM – cell biological applications

TIRFM: GLUT4 vesicles near or at the plasma membrane

EPI-IF: inserted into the plasma membrane



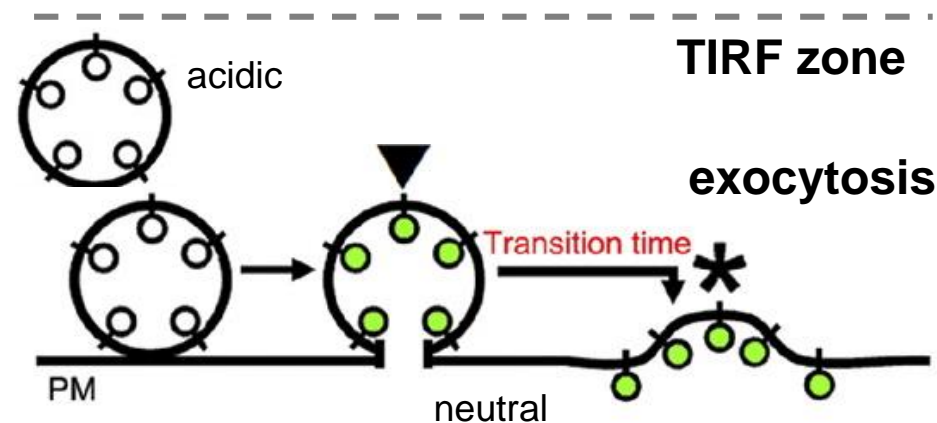
HA-GLUT4-GFP fluorescence in basal or insulin-stimulated adipocytes

The TIRF assay measures redistribution to within 250 nm of the PM independently of whether the GLUT4 is inserted into the PM (that is, independently of vesicle fusion). **GFP = in the vicinity and inserted into the plasma membrane**

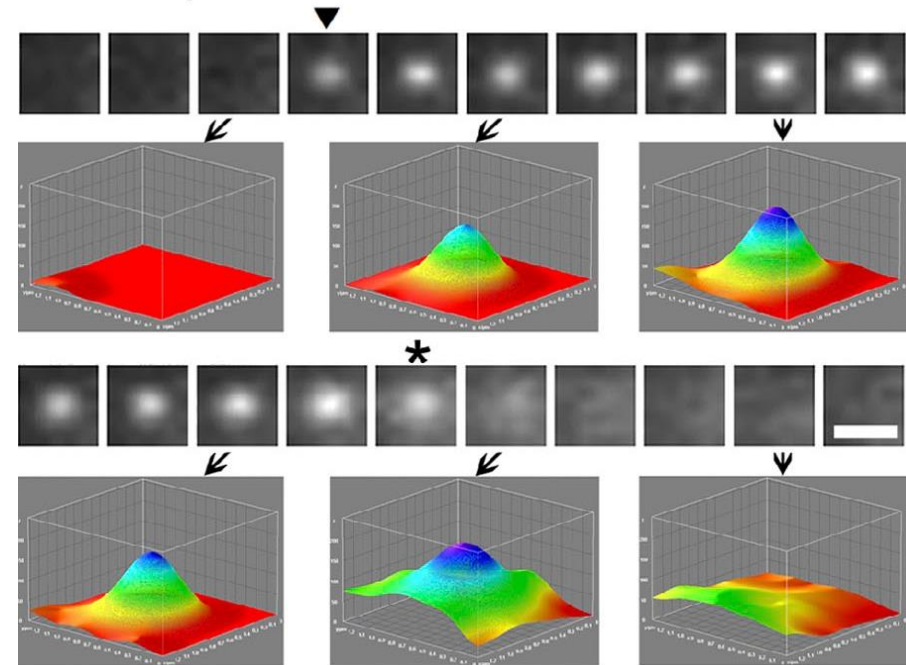
In the epifluorescence mode, translocation is measured as the exposure of the HA-epitope of HAGLUT4-GFP on the surface of intact adipocytes, which is measured by IF. **CY3 = inserted into the plasma membrane**

TIRFM – cell biological applications

TIRFM: VAMP2-pHluorin: pHluorin is a pH-sensitive fluorescent protein that becomes much more fluorescent when transferred from an acidic (enclosed in the vesicle lumen) to a neutral (vesicle opens) environment

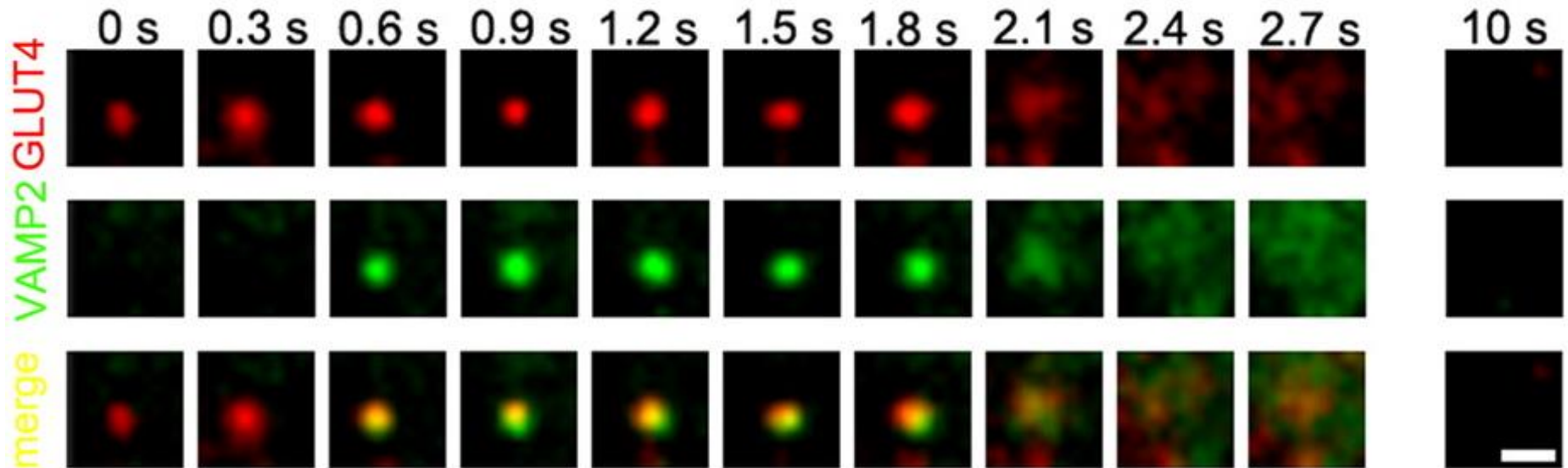
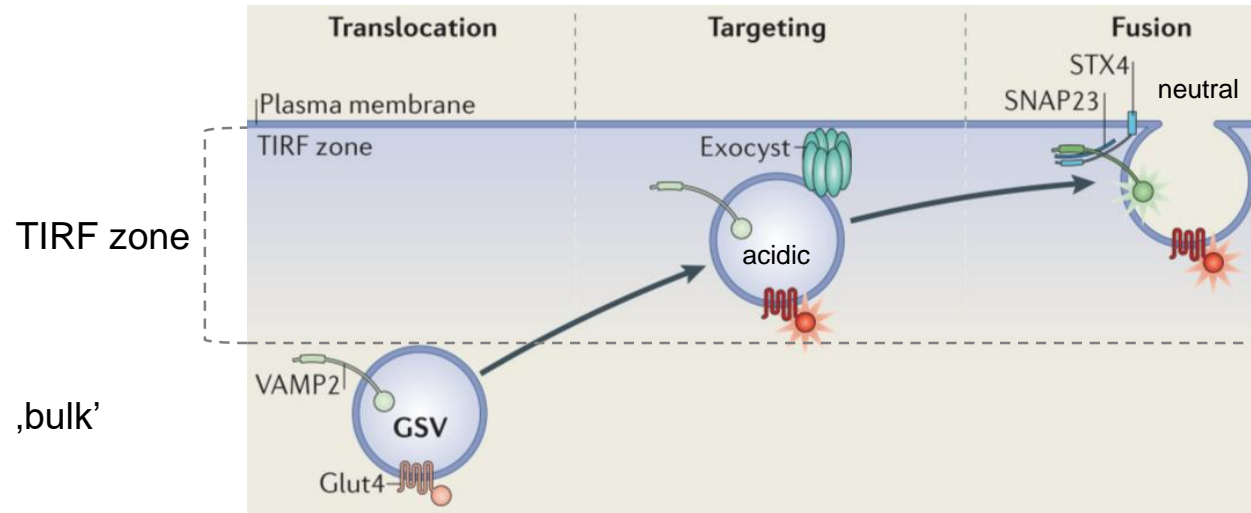


VAMP2-pHluorin



VAMP2-pHluorin fluorescence appears, brightens upon fusion pore formation, and then spreads laterally as the vesicle collapses into the PM

TIRFM – cell biological applications



3T3-L1 adipocytes, VAMP2-pHluorin: pHluorin is a pH-sensitive fluorescent protein that becomes much more fluorescent when transferred from an acidic to a neutral environment; GFP-GLUT4

Xu, Y. *et al.* Dual-mode of insulin action controls GLUT4 vesicle exocytosis. *J. Cell Biol.* **193**, 643–653 (2011)

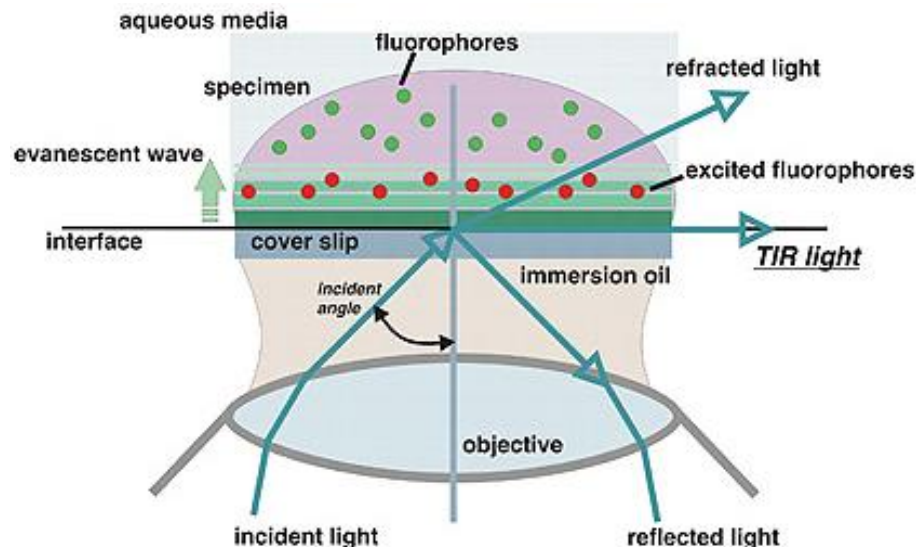
Leto D. *et al.* Regulation of glucose transport by insulin: traffic control of GLUT4. *Nature Reviews Molecular Cell Biology* **13**, 383–396 (2012)

TIRFM – EVANESCENT WAVE ILLUMINATION

TIRFM, AS A NEAR-FIELD IMAGING METHOD PROVIDES A SURFACE-SELECTIVE ILLUMINATION AND RESOLUTION IMPROVEMENT DUE TO THE UNIQUE PROPERTIES OF THE EVANESCENT FIELD.

EVANESCENT WAVE

- decays exponentially in intensity with increasing distance normal to the surface
- decay length (d) is in the order of the wavelength of the incident light (λ)
- selectively excites fluorophores very near to a solid surface (~ 100 nm)
- eliminates background fluorescence from out-of-focus planes, improves SNR



CYTOSKELETAL DYNAMICS GROUP



University of Pécs - Medical School
Department of Biophysics

THE TEAM

PUBLICATIONS

RESEARCH

FUNDING

for STUDENTS

CONTACT

THANK YOU FOR YOUR ATTENTION!

<http://cytoskeletaldynamics.wix.com/mysite>

<http://biofizika.aok.pte.hu>

Post-docs

Tamás Huber
Andrea Vig
Péter Bukovics



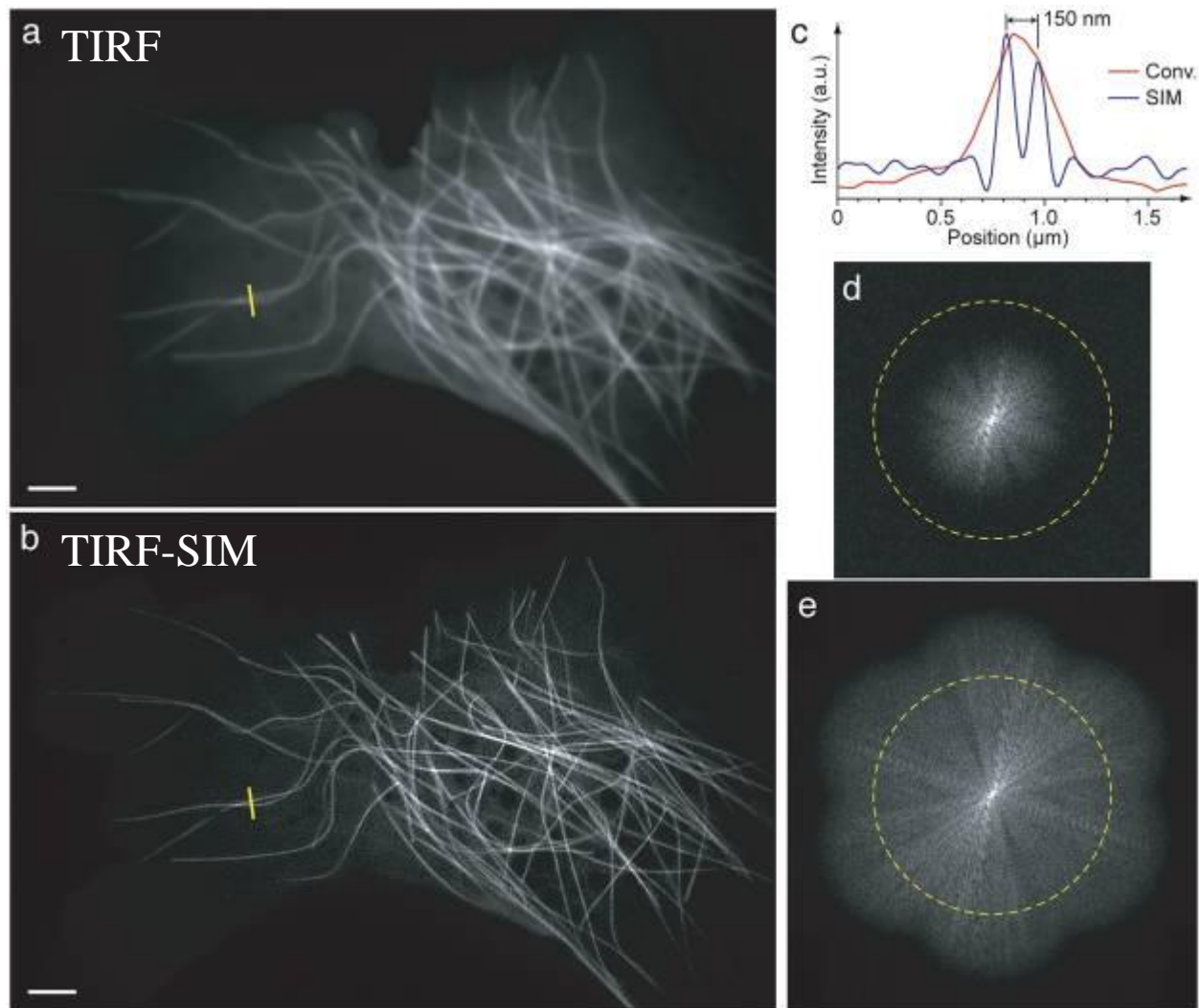
PhD Students

Réka Pintér
Mónika Tóth
Veronika Kollár
Rauan Shakenov



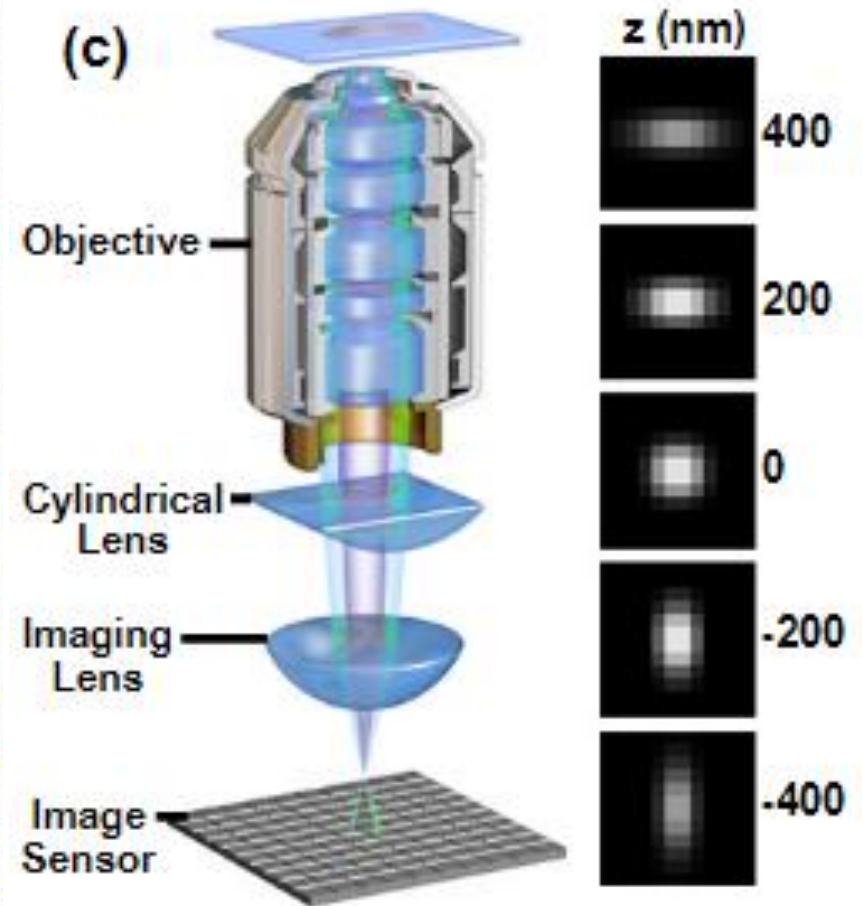
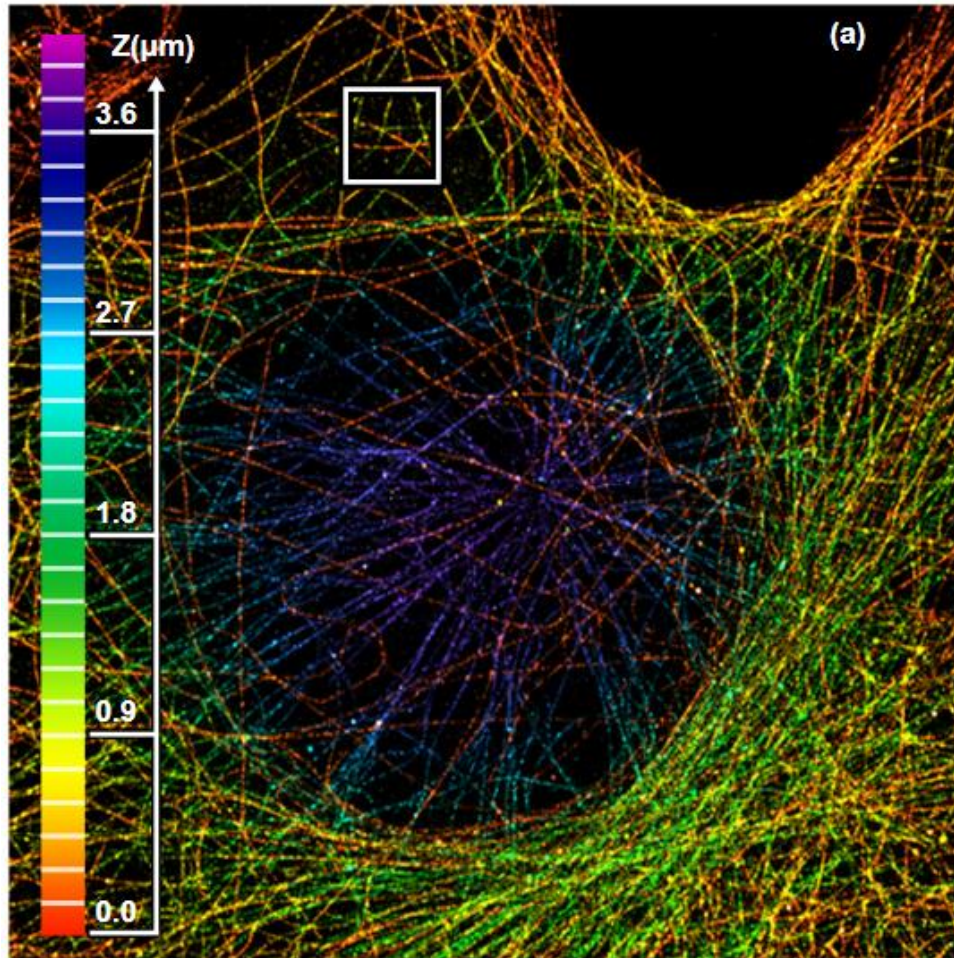
Péter Gaszler



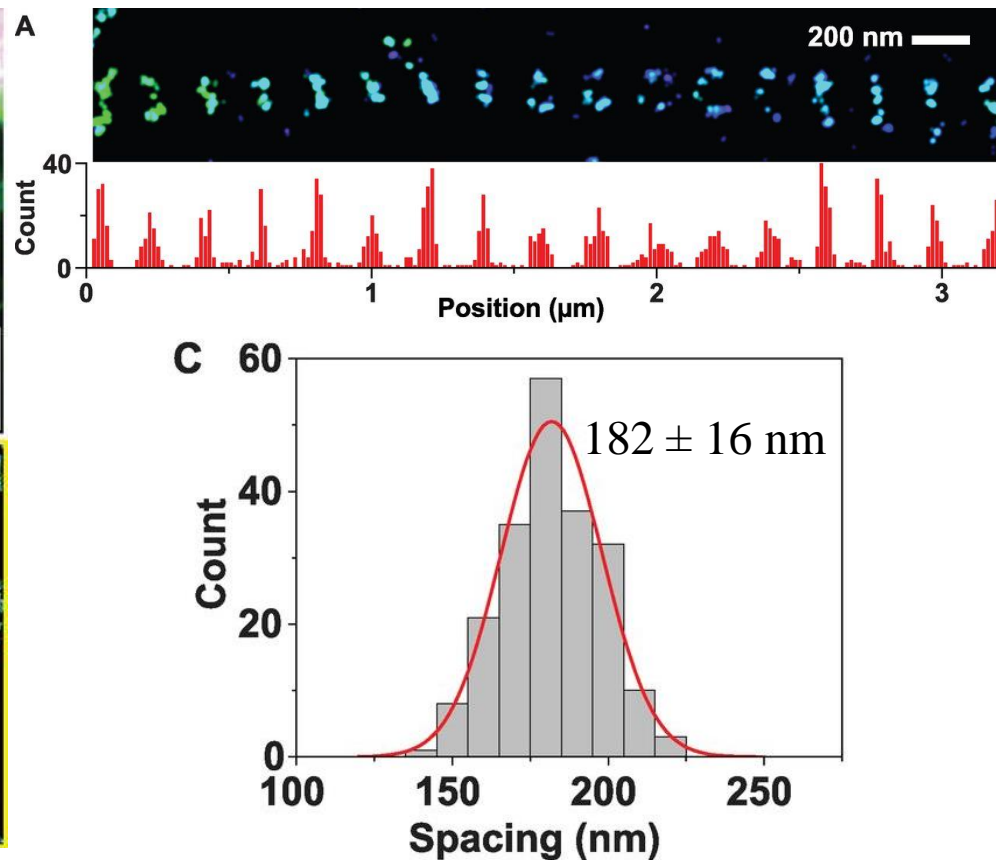
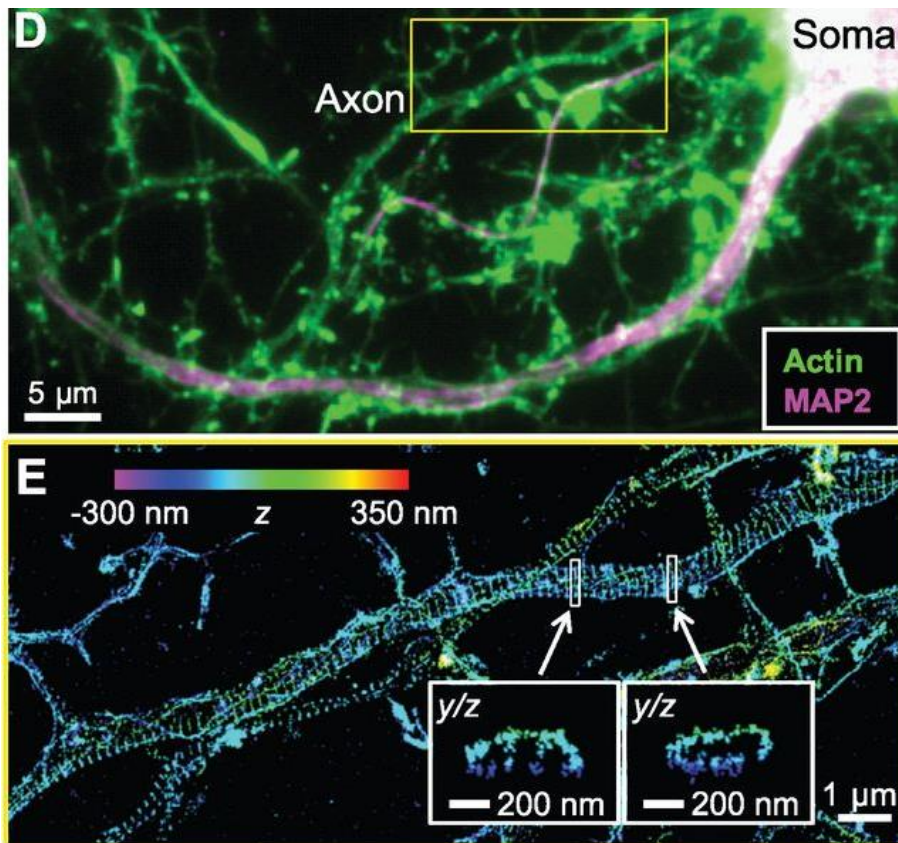


Comparison of conventional TIRF (**a**) and TIRF-SIM (**b**) images of the microtubule cytoskeleton in a single S2 cell. Scale bar $2 \mu\text{m}$. (**c**) Normalized intensity profiles along the yellow lines in (**a**) (red curve) and (**b**) (blue curve). Two microtubules separated by $\sim 150 \text{ nm}$ are well resolved in the SIM reconstruction, but not by conventional microscopy. (**d–e**) Fourier transforms of the images in (**a**) and (**b**) respectively. The classical diffraction limit of the objective lens is indicated by a dashed circle of radius $5.96 \mu\text{m}^{-1}$.

P. Kner, B.B. Chhun, E.R. Griffis, L. Winoto, M.G.L. Gustafsson *Super-resolution video microscopy of live cells by structured illumination*. *Nature Methods* vol.6, p.339–342 (2009) Brief Communication



3D STORM image of a BSC-1 cell stained for alpha-tubulin with Alexa Fluor 647 (Nikon N-STORM 4.0). The bar on the left provides the z position in micrometers (μm) corresponding to each color in the image. (c) Graphic illustrating the 3D STORM principle. A **cylindrical lens introduces astigmatism, causing the image of single emitters to be stretched in the x or y directions as a function of z position.** Correlation of the magnitude and direction of stretching with a calibration file allows determination of the z position with high precision.



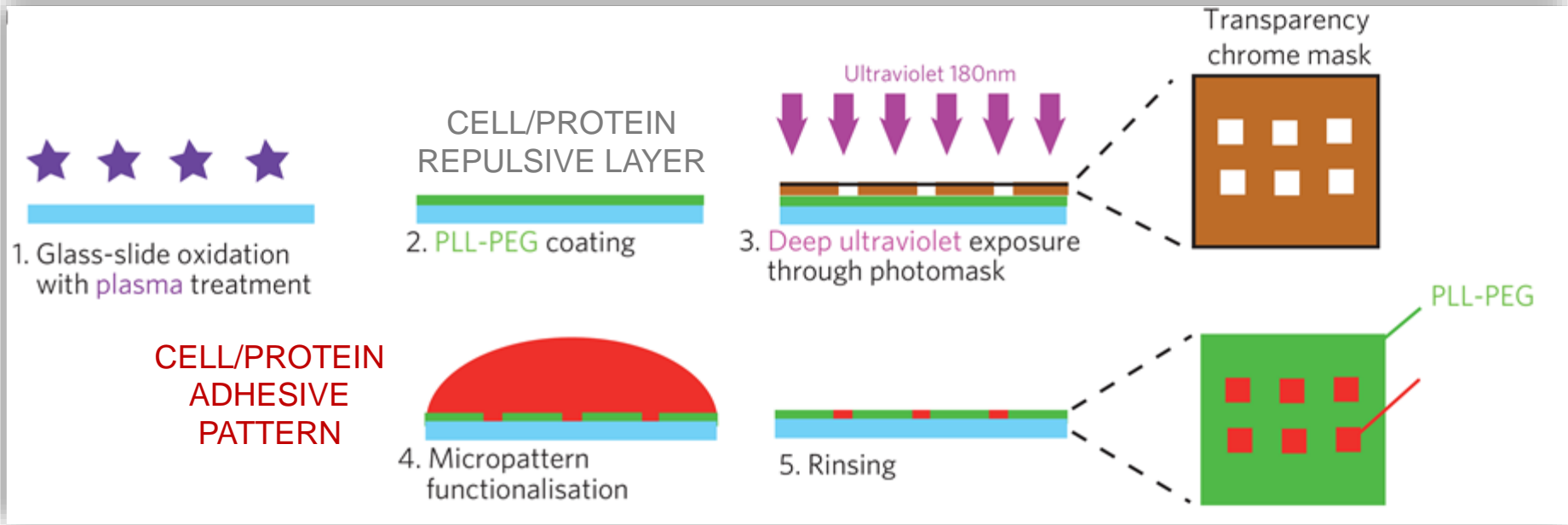
Actin filaments in axons form a quasi-1D, periodic structure with a uniform spacing of ~180 to 190 nm.

(D) Conventional fluorescence image of actin (green) and MAP2 (dendritic marker, magenta) in a neuron fixed at 12 DIV. (E) 3D STORM image of actin in a region containing axons (devoid of the MAP2). The yz cross sections corresponding to the white-boxed regions are shown.

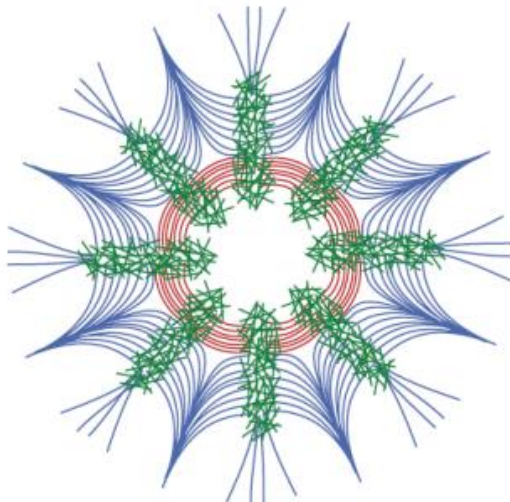
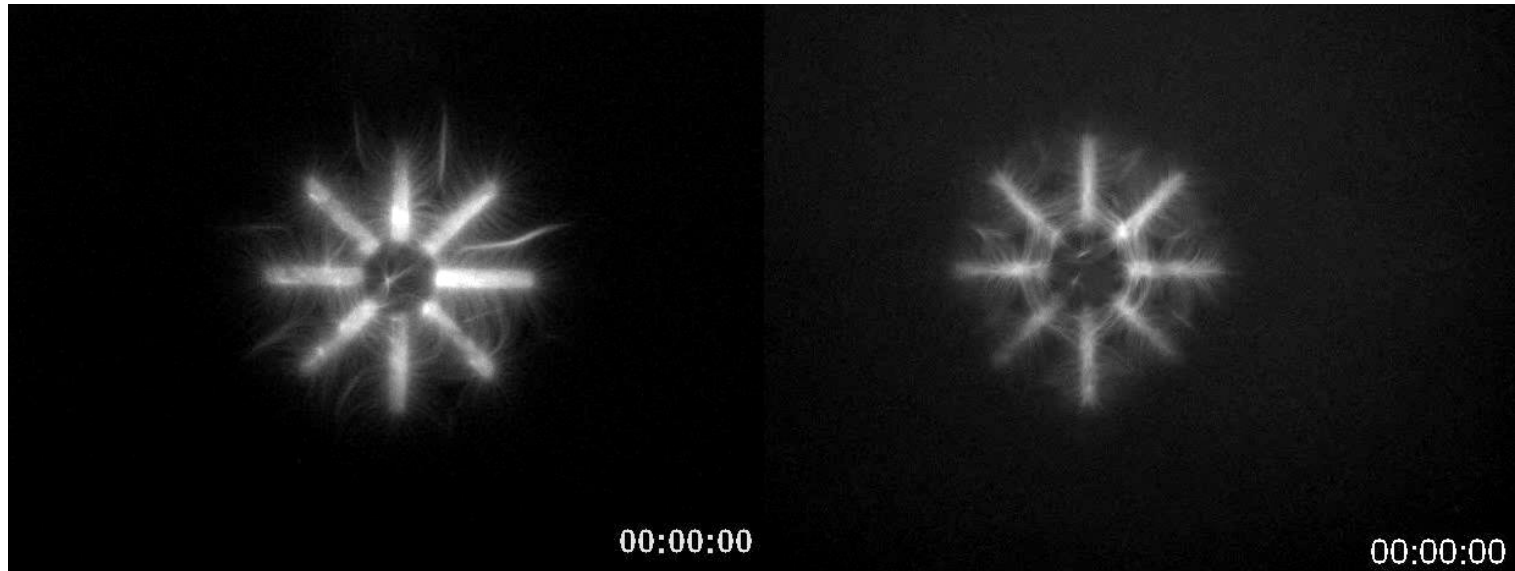
(A) Three-dimensional STORM image of a segment of axon (top) and the **distribution of localized molecules** after the 3D image was projected to one dimension along the axon long axis (bottom). (C) Histogram of the spacings between adjacent actin ringlike structures (N = 204 spacings). The red line is a Gaussian fit with a mean of 182 nm and a SD of 16 nm.

TIRFM - MICROPATTERNING

Laurent Blanchoin: NRS, BIG/DRF/CEA,
Cytomorpholab Grenoble



Nucleation geometry governs ordered actin networks structures



ANGLE (direction!)
BETWEEN FILAMENTS

Actin filaments :

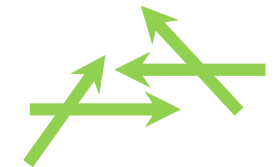
anti-parallel 
parallel 

branched meshwork 

PARALLEL



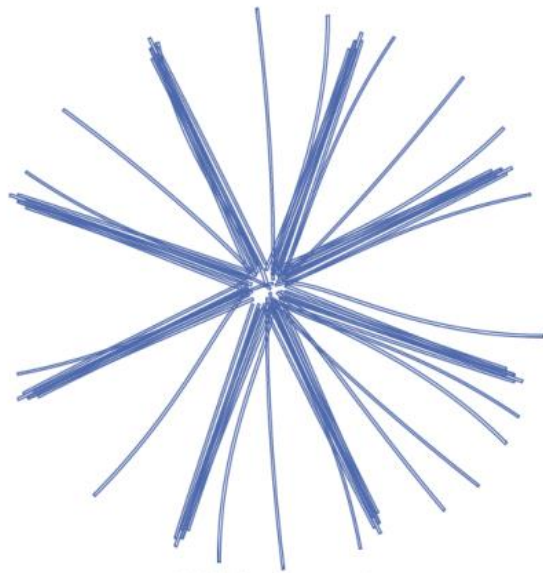
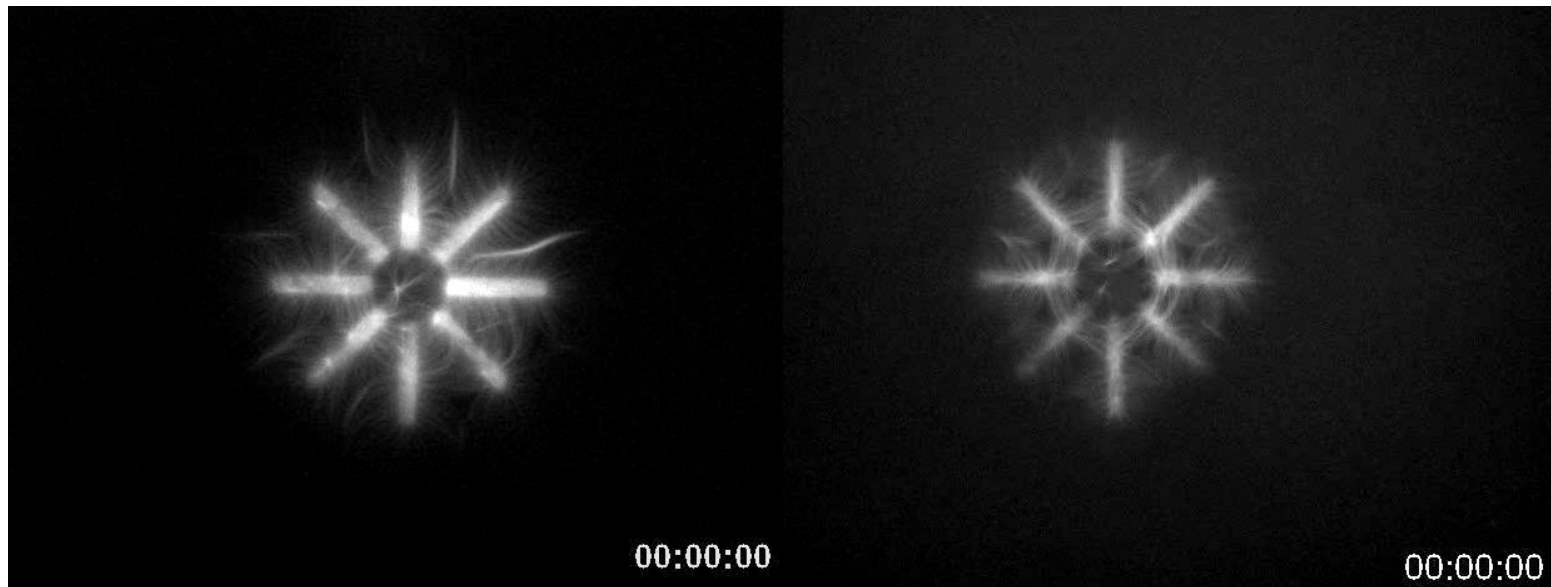
BRANCHED



ANTIPARALLEL



Actin network architecture can determine myosin motor activity



ANGLE (direction!)
BETWEEN FILAMENTS

Actin filaments :

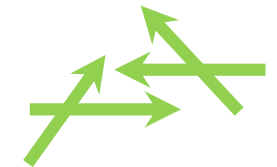
anti-parallel 
parallel 

branched
meshwork 

PARALLEL



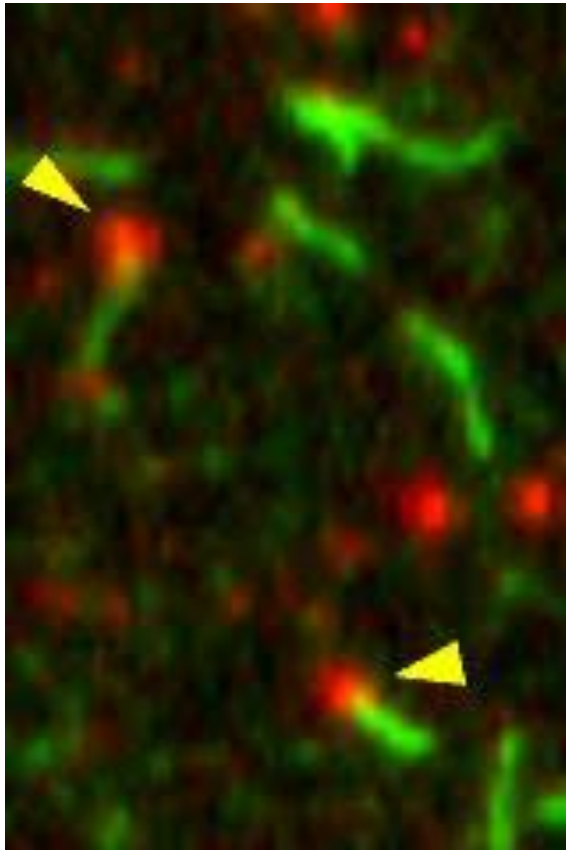
BRANCHED



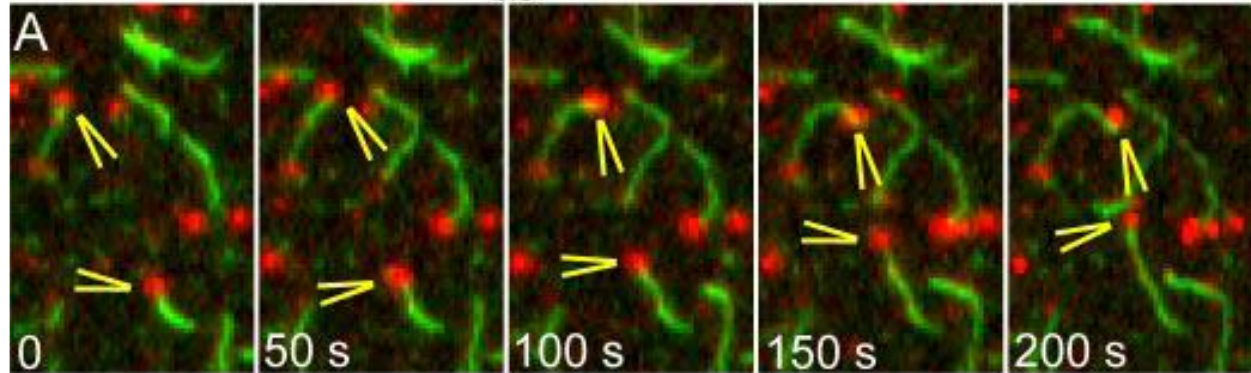
ANTIPARALLEL



Formin proteins track the growing barbed ends of actin filaments – processive actin polymerase



18 nM QD-Bni1(FH1FH2) p_{bio} + 1.5 μM Actin

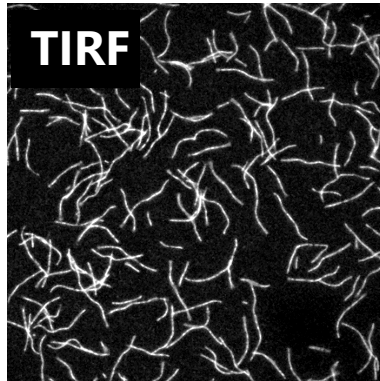
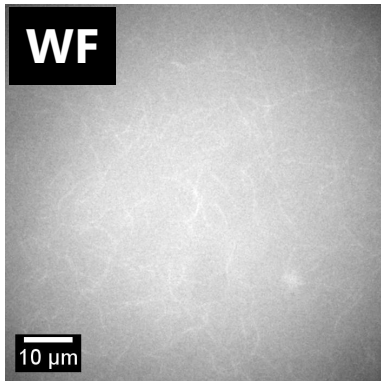


Courtesy: Paul A., Pollard T.C. JBC 2009

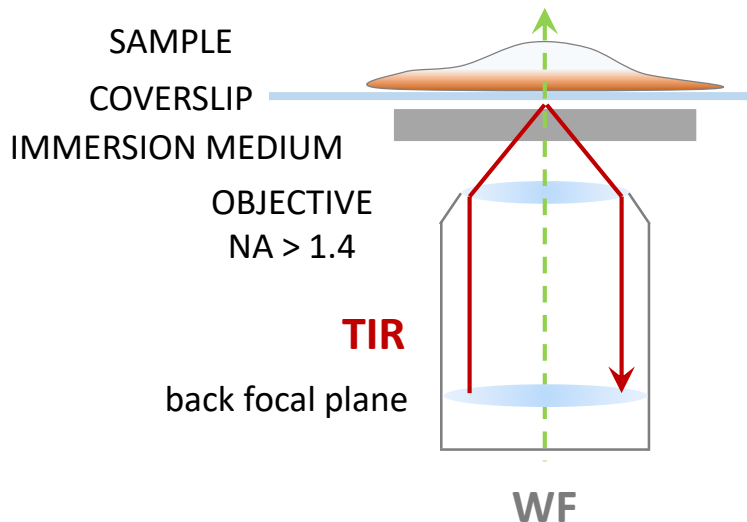
FORMIN: QDot 625 nanocrystal
ACTIN: Alexa488

STUDYING THE DYNAMIC BEHAVIOUR OF ACTIN

DIRECT „OBSERVATION” OF ABPs ACTIVITIES

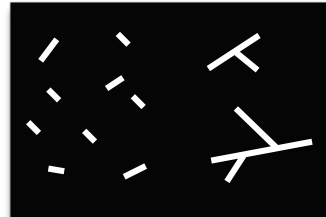


**OBJECTIVE BASED
TIRFM**



SPONTANEOUS ACTIN DYNAMICS

$k_+, k_-, [G], [F]$



NUCLEATION FACTORS

$[F], k_+, k_-$

e.g. formins, Arp2/3 complex



SEQUESTRATORS

$[G], [F]$

e.g. WH2 domain proteins



ELONGATION/CAPPING FACTORS

k_+, k_-

e.g. formins, VASP, CP



FILAMENT BINDING

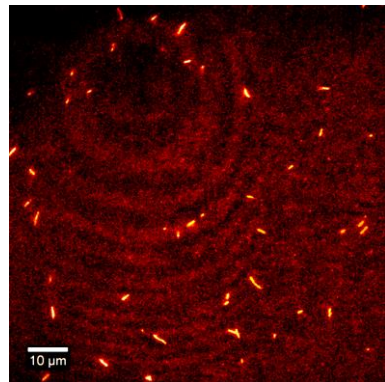
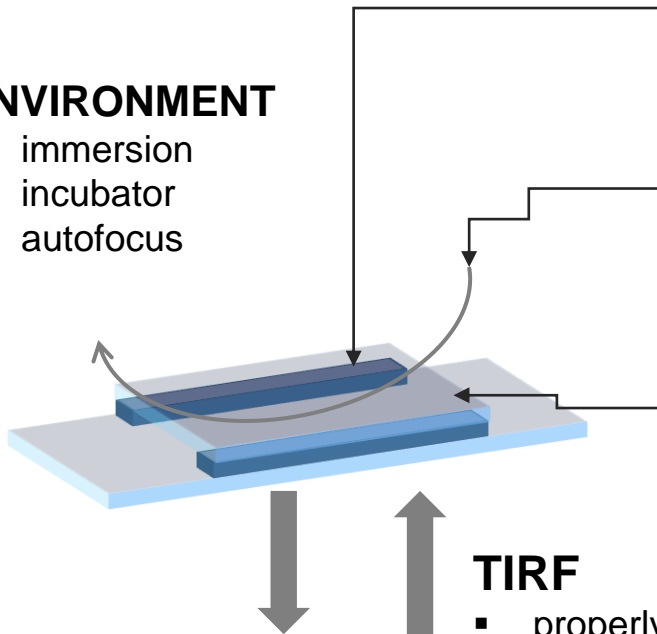
$k_+, k_-, [F]$

severing, stabilization

Sample preparation

ENVIRONMENT

- immersion
- incubator
- autofocus



TIRF

- properly aligned laser beam
 - no optical imperfections
 - properly mounted coverslip (no tilt!)
-
- interference fringes
 - inhomogeneous field

SAMPLE (cells, proteins, ...)

- fluorescently labeled, no restriction of usable fluorophores (!available wavelength, and filter set)
- oxygen scavenger system
- low refractive index medium

FLOW CELL

- manual / microfluidics

SURFACE CHEMISTRY

- poly-L-lysine (PLL)
- collagen/fibronectin
- PLL-g-PEG
- streptavidine-biotin
- NEM-myosin

